

# c0004 Cyclostratigraphy and Astrochronology

L.A. Hinnov and F.J. Hilgen

## Chapter Outline

4.1. Introduction	63	4.7.2. Tidal Dissipation, Dynamical Ellipticity and Climate Friction	74
4.2. Earth's Astronomical Parameters	64	4.7.3. Solar System Diffusion	76
4.3. The 405-kyr Metronome	67	4.7.4. Summary of Uncertainties	76
4.4. Astronomically Forced Insolation	67	4.8. Astrochronology-Geochronology Intercalibration	76
4.5. Cyclostratigraphy through Geologic Time	67	4.9. A New Astronomical Solution	78
4.6. Constructing Astrochronologies and the ATS	71	References	78
4.7. Precision and Accuracy of the ATS	72		
4.7.1. Seasonal Phase Relations	72		

## s0010 4.1. INTRODUCTION

p0015 Paleoclimatological research has led to wide acceptance that quasi-periodic oscillations in the Sun-Earth position, known as *Milankovitch cycles*, have induced significant variations in Earth's past climate. These astronomically forced climate variations have in turn influenced climate-sensitive sedimentation, and thereby came to be fossilized in the Earth's cyclic stratigraphic, or cyclostratigraphic record. The sub-discipline that has developed to study this record is known today as *cyclostratigraphy*. The detection of astronomical signals in cyclostratigraphy has been facilitated by impressive advancements in celestial mechanics, which have provided accurate models of Earth's orbital-rotational behavior through geological time, and also by equally notable improvements in data collection and analysis.

p0020 A principal outcome of these developments has been the recognition that the cyclostratigraphic record, when shown to carry a signal specific to Earth's astronomical parameters, serves as a powerful chronometer. The astronomical calibration of these cycles leads to *astrochronology* and construction of the *Astronomical Time Scale (ATS)*. High quality data from the Cenozoic Era have demonstratively preserved all of the astronomical cycles predicted by modern celestial mechanics; the Neogene and Paleogene periods are now almost completely astronomically calibrated, as reported in Chapters 28 and 29, although serious

problems remain in the Paleogene. Cyclostratigraphy from more remote geological ages cannot be calibrated fully or directly to the astronomical variations, because of model limitations and uncertainties in determining stratigraphic age. Nonetheless, in numerous instances signals analogous to those of the modeled astronomical variations have been detected in cyclostratigraphy, prompting the development of "floating" astrochronologies over extended time intervals (multiple millions of years). Astronomically calibrated floating time scales have now been proposed for intervals that extend through entire stages in the Triassic, Jurassic and Cretaceous periods, and are presented in Chapters 25, 26 and 27.

This chapter provides an introduction to the Earth's p0025 astronomical parameters, the nature of the astronomically forced incoming solar radiation (insolation), and the discovery of astronomically forced insolation signals in cyclostratigraphy. For remote geologic times, partial astronomical calibration with the modeled 405-kyr orbital eccentricity variation is allowable; the construction and application of the "405-kyr metronome" is explained. This is followed by a summary of the cyclostratigraphy that was used in the "absolute" and "floating" astrochronologies of the Geologic Time Scale 2012 (GTS2012). A discussion of the precision and accuracy that can be expected from astronomically calibrated cyclostratigraphy is also given. The chapter concludes with remarks on recent inter-calibration efforts between

astrochronology and geochronology — the key to future improvement in geologic time scale determination.

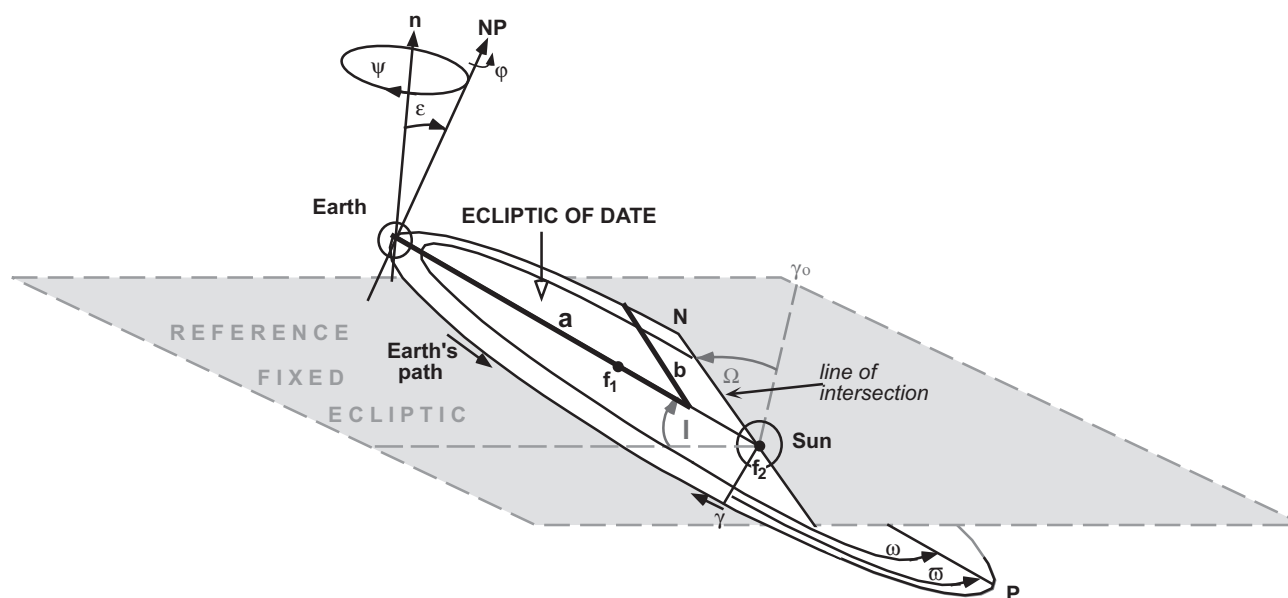
## s0015 4.2. EARTH'S ASTRONOMICAL PARAMETERS

p0030 The Earth undergoes quasi-periodic changes in its orientation relative to the Sun, as a consequence of interactions between the Earth's axial precession and variable orbit induced by motions of the other planets. These changes may be described in terms of the Earth's astronomical parameters (Figure 4.1). Quantification of these parameters has been carried out numerous times in the past using analytical approximations of the planetary motions; a brief history of these computations is given in Laskar et al. (2004). Today, models of the astronomical parameters are based on computerized numerical integration, and include important new variables, e.g., relativistic effects, flattening of the Earth, Sun and Moon, Earth's tidal deceleration, climate friction, and other factors. The nominal La2004 model includes all of the above-mentioned variables, and provides an accurate orbital eccentricity model back to 40 Ma (Laskar et al., 2004). A new La2010 solution extends accuracy back to 50 Ma (Section 4.9). Further back in time, however,

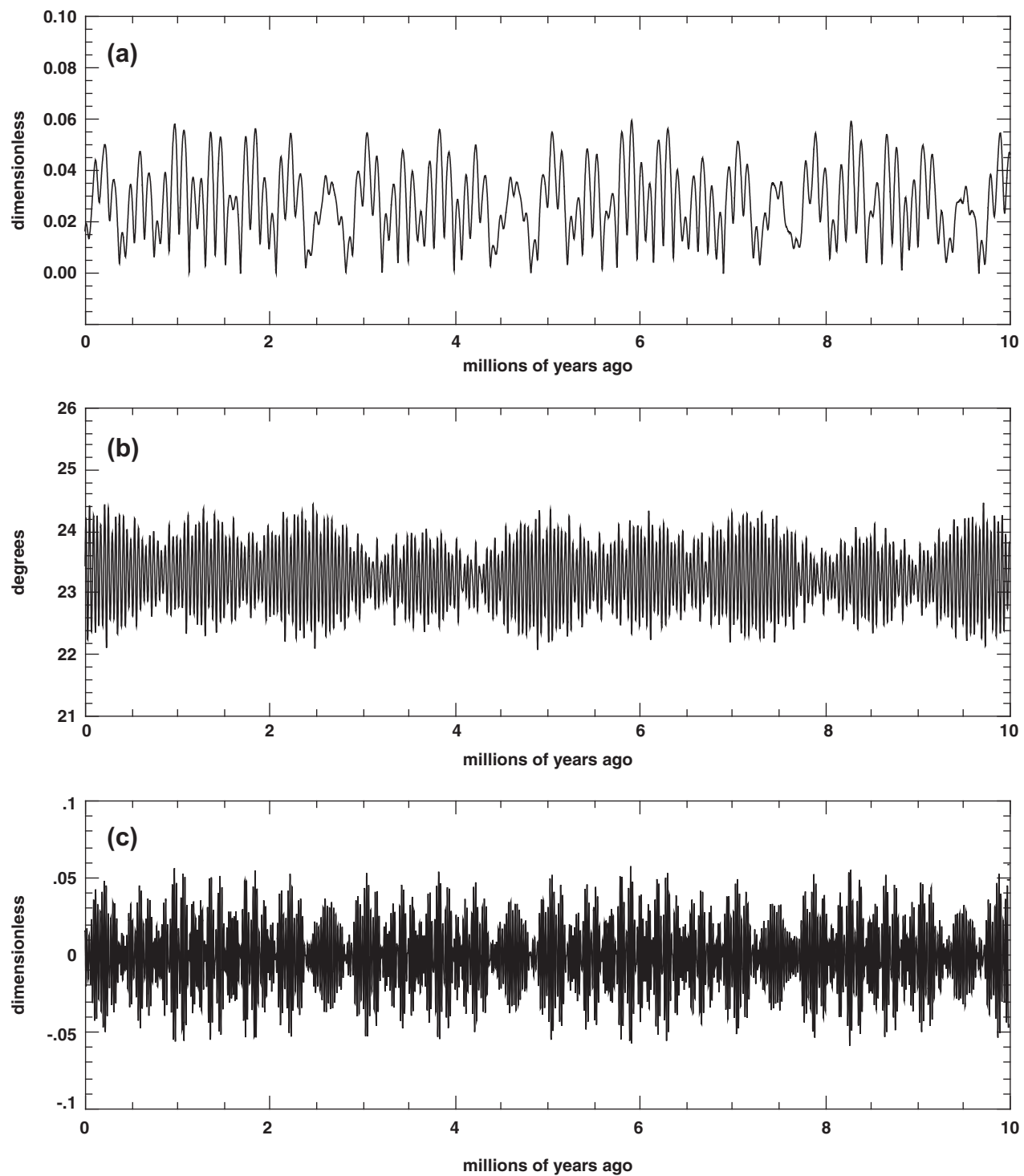
modeling validity rapidly diminishes due to uncertainties in model initial conditions and numerical integration error. While the initial conditions can be improved, integration error ultimately limits the validity of the model to approximately 60 Ma (Laskar, 2006).

Over the past 10 million years the Earth's *orbital eccentricity* has varied between 0–0.07 (Figure 4.2a) with principal periods at 95 kyr, 99 kyr, 124 kyr, 131 kyr, 405 kyr, and 2260 kyr (Figure 4.3a), caused by gravitational perturbations from the motions of the other planets acting on Earth's orbital elements  $\Pi$  and  $e$  (Figure 4.1). The *obliquity* variation changes the Earth's axial tilt by between  $22^\circ$ – $24^\circ$  (Figure 4.2b), with a principal period at 41 kyr, and lesser ones at 39 kyr, 54 kyr and 29 kyr (Figure 4.3b), due to planetary motions acting mainly on orbital elements  $I$  and  $\Omega$  (Figure 4.1). The *precession index* represents the combined effects of orbital eccentricity and the Earth's axial precession on the Sun-Earth distance (Figure 4.2c), and has principal periods at 24 kyr, 22 kyr, 19 kyr and 17 kyr (Figure 4.3c).

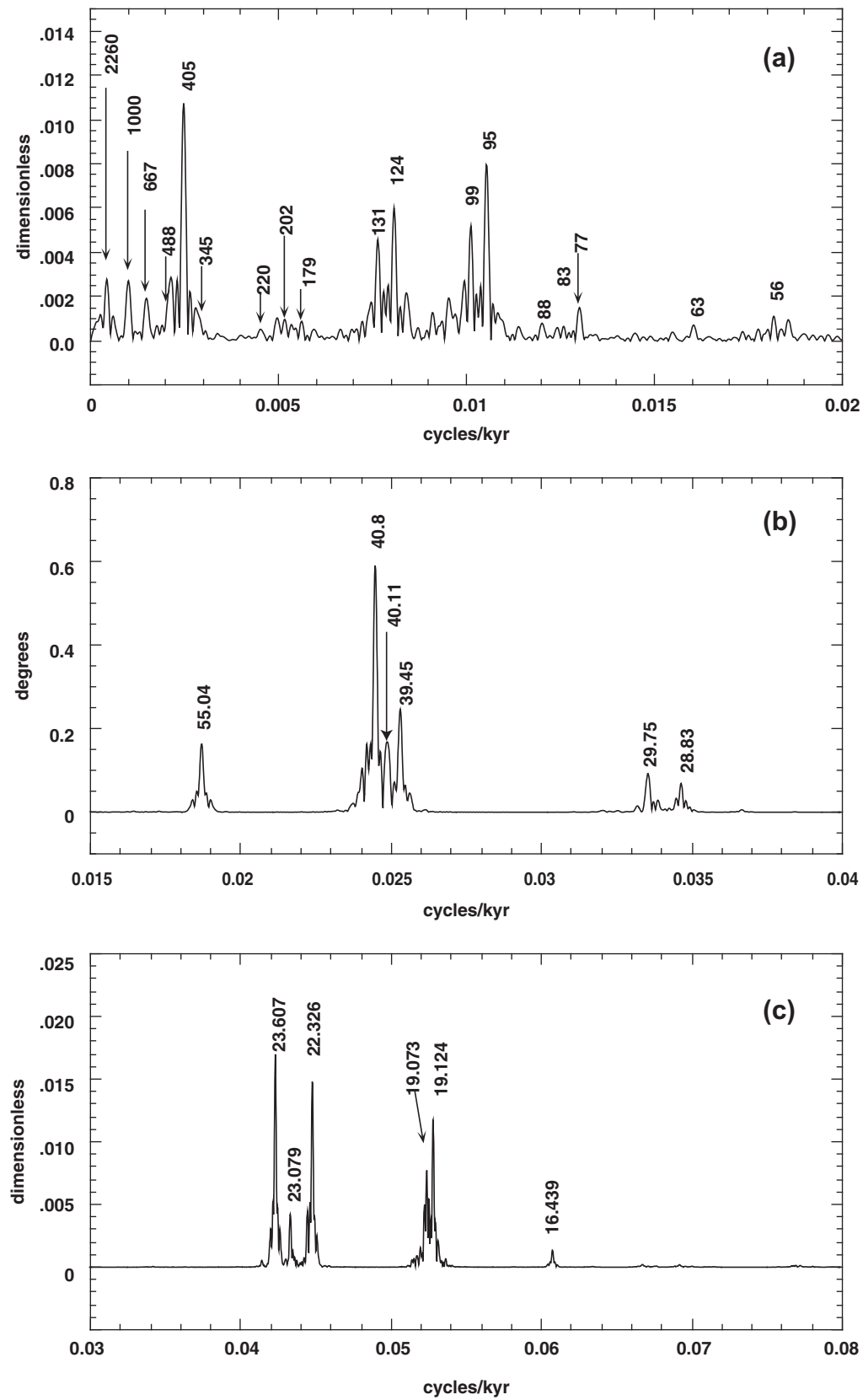
Long-term secular changes in geophysical and astrodynamical factors are expected to have influenced the frequencies and phasings of the astronomical parameters. These factors include chaotic diffusion of the Solar System, tidal dissipation of the Earth-Moon system, Earth's dynamical ellipticity and climate friction (Section 4.7). At present



f0010 **FIGURE 4.1** The Earth's astronomical parameters viewed from above the Earth's geographic North Pole (NP) in a configuration of northern summer solstice (NP pointed towards the Sun). The Earth's orbit is elliptical with (invariant) semi-major axis  $a$  and semi-minor axis  $b$  defining eccentricity  $e$ . The Sun occupies one of the two foci ( $f_1$ ,  $f_2$ ). Variables  $e$ ,  $\Pi$ ,  $I$  and  $\Omega$  are "orbital elements," where  $\Pi = \Omega + \omega$ . The plane of the Earth's orbit (the "ecliptic of date") is inclined at an angle  $I$  relative to the fixed reference ecliptic, and intersects this reference ecliptic at a longitude  $\Omega$  at point N, the ascending node, relative to fixed vernal point  $\gamma_0$ . (In this depiction,  $I$  is greatly exaggerated from its actual magnitude of 1 to  $2^\circ$ .) The orbital perihelion point P is measured relative to  $\gamma_0$  as the longitude of perihelion  $\Pi$ , and moves slowly anticlockwise. The Earth's figure is tilted with respect to the ecliptic of date normal  $n$  at obliquity angle  $\epsilon$ . Earth's rotation  $\phi$  is anticlockwise; gravitational forces along the ecliptic of date from the Moon and Sun act on the Earth's equatorial bulge and cause a clockwise precession  $\psi$  of the rotation axis. This precession causes the vernal equinox point  $\gamma$  to migrate clockwise along the Earth's orbit, shifting the seasons relative to the orbit's eccentric shape; this motion constitutes the "precession of the equinoxes." The angle  $\omega$  between  $\gamma$  and P is the moving longitude of perihelion and is used in the precession index  $e \sin \omega$  to track Earth-Sun distance. Variations of  $e$ ,  $\epsilon$  and  $e \sin \omega$  are shown in Figure 4.2.



f0015 **FIGURE 4.2** Variations of the Earth's astronomical parameters over the past 10 million years according to the nominal La2004 model sampled at 1-kyr intervals (Laskar et al., 2004). (a) Orbital eccentricity (dimensionless). (b) Obliquity variation, in degrees of axial tilt. (c) Precession index (dimensionless). All values may be downloaded from the website: <http://www.imcce.fr/Equipes/ASD/insola/earth/earth.html>.



f0020 **FIGURE 4.3** Harmonic analysis using  $4\pi$  multi-tapers (Thomson, 1982) of the Earth's astronomical parameters depicted in Figure 4.2. Labels identify periodic components in thousands of years. (a) Orbital eccentricity. (b) Obliquity variation. (c) Precession index. Due to the quasi-periodic nature of the parameters and other factors (Section 4.7), the significance, periodicity and amplitude of the labeled components may change for analyses performed over other time segments.

the effects of these factors are in the main known only theoretically; the cyclostratigraphic record has yet to be analyzed for the magnitude and timing of these factors.

### s0020 4.3. THE 405-KYR METRONOME

p0045 While chaotic behavior has in all likelihood affected Earth's ~100 kyr scale orbital eccentricity terms through geologic time, the 405 kyr eccentricity cycle has remained relatively stable over at least the past 250 million years (Laskar et al., 2004). This high-amplitude cycle is the consequence of gravitational interactions between Jupiter and Venus, i.e., motions of their orbital perihelia,  $g_2-g_5$ . The large mass of Jupiter is responsible for the stability of the 405-kyr cycle, which has an estimated uncertainty of ~500 kyr at 250 Ma. Thus, this cycle can be used as a basic calibration period for cyclostratigraphy; this approach has been advocated by Laskar et al. (2004), and many others. Today 405-kyr cyclicity has been recognized in many cyclostratigraphic sequences, as demonstrated in the astrochronologies presented in Chapters 25–29 of this volume. It now appears that many of the so-called “third order sequences” in Mesozoic stratigraphy are responses to the 405-kyr eccentricity cycle through climate forcing by precession index carriers (e.g., Gale et al., 2002; Boulila et al., 2010a).

p0050 To obtain the 405-kyr metronome, Laskar et al. (2004) suggested using the simple formula:  $e_{405} = 0.027558 - 0.010739 \cos(2434^\circ + 3.200^\circ t)$ . However, this formula is valid only for 0–100 Ma. To provide an accurate metronome for the entire modeled 0–249 Ma, the nominal La2004 orbital eccentricity series was down-sampled to an 8 kyr spacing (down from 1 kyr given by Laskar et al., 2004); bandpass filtering was applied to extract the 405-kyr cycle. The filtered signal (normalized to unity) is the 405-kyr metronome; four representative time slices are shown in Figure 4.4. The depicted single-frequency metronome has been included in *TSCreator* (Ogg, et al., 2011). The long-term goal of astrochronology is to assign (“tune”) cyclostratigraphy to the appropriate 405-kyr bins.

p0055 A slightly wider passband surrounding the 405-kyr term includes the important  $g_4-g_3$  modulation into the metronome (Laskar et al., 2011). Figure 4.4 also displays this wide-band metronome, which can vary significantly from the single-frequency metronome. The wide-band metronome can be used to accurately tune cyclostratigraphy over 0–40 Ma using La2004, and over 0–50 Ma using La2010 (Section 4.9). Prior to 50 Ma, however, the  $g_4-g_3$  modulation is inaccurately known (Section 4.7); for Mesozoic and older cyclostratigraphy the single-frequency metronome should be assumed.

### s0025 4.4. ASTRONOMICALLY FORCED INSOLATION

p0060 The orbital parameters affect changes in the intensity and timing of the incoming solar radiation, or insolation, at all

points on the Earth. When considered at interannual time scales, these insolation changes comprise the well-known Milankovitch cycles (Milankovitch, 1941; reissued in English in 1998). Figure 4.5 compares Milankovitch's original calculation of northern summer insolation at 65°N with a modern calculation based on La2004. Geographical location, time of year, and even the time of day all determine the relative contributions of the orbital parameters to the inter-annual insolation (e.g., Berger et al., 1993; Berger et al., 2010). For example, Figure 4.6 depicts the globally available spectral power of orbitally forced daily insolation at the top of the atmosphere on June 21 (solstice) and March 21 (equinox). These examples are idealized in the sense that it is unlikely that climate responds to insolation on only one day of the year, but rather integrates insolation over certain times of the year and collectively over specific geographic areas, possibly over different areas at different times. This “climatic filtering” alters the relative contributions of the orbital parameters to the total output climate response, this even prior to internal climate system responses to the insolation. Thus, it is left to the discretion of the paleoclimatologist to determine which time(s) of the year and at which location(s) a prevailing climate has responded to insolation; this can require considerable insight into the infinite number of ways that one can sample insolation in space-time (Rubincam, 1994).

### 4.5. CYCLOSTRATIGRAPHY THROUGH GEOLOGIC TIME s0030

The prospect that Earth's astronomical variations have exerted large-scale climatic changes that could be detected in the geologic record was already being debated in the 19<sup>th</sup> century (e.g., Herschel, 1830; Adhémar, 1842; Lyell, 1867; Croll, 1875). Early attempts to link astronomical effects to paleoclimate are reviewed in Hilgen (2010). Gilbert (1895) was the first to attribute the origin of limestone/shale cyclic strata of the Cretaceous Niobrara chalks (Colorado, USA) to astronomical forcing. Bradley (1929) counted varves in the lacustrine oil shale/marl cycles of the Eocene Green River formation (Utah, USA) estimating an average 21,630-year time scale for the cycles, and pointing to the precession of the equinoxes as a potential cause. The first correlation between astronomically calculated insolation minima and Late Quaternary ice age deposits of the Alps was made by Köppen and Wegener (1924), who used insolation as calculated by Milankovitch for critical latitudes and seasons (i.e., similar to 65°N Summer); this correlation and tuning was also discussed at length in Milankovitch (1941). Milankovitch (1941) was the first to attempt a quantitative correlation between astronomically calculated insolation minima and Late Quaternary ice age deposits of the Alps. However, later radiocarbon studies of glaciation timings in North America did not clearly corroborate Milankovitch's insolation

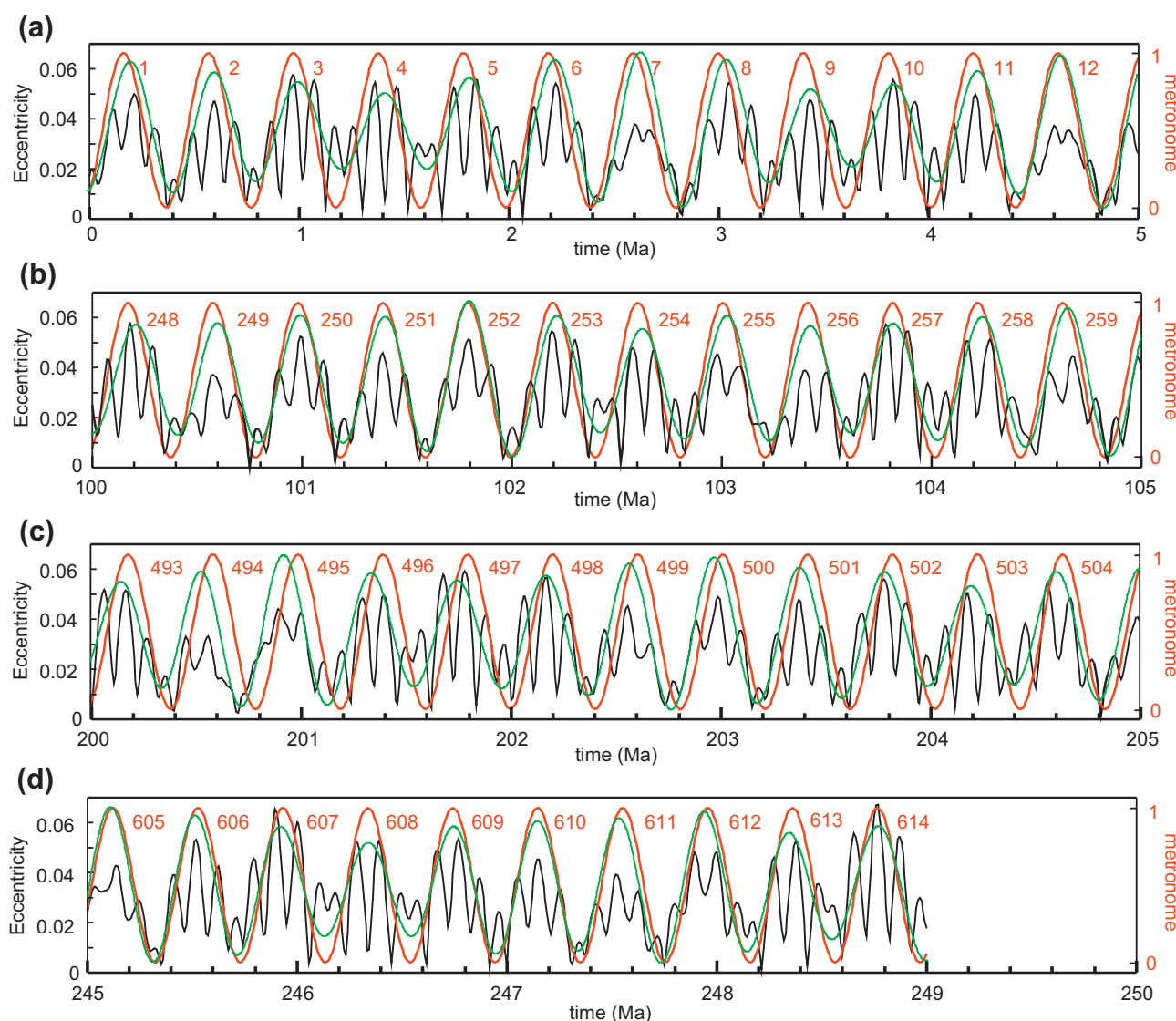


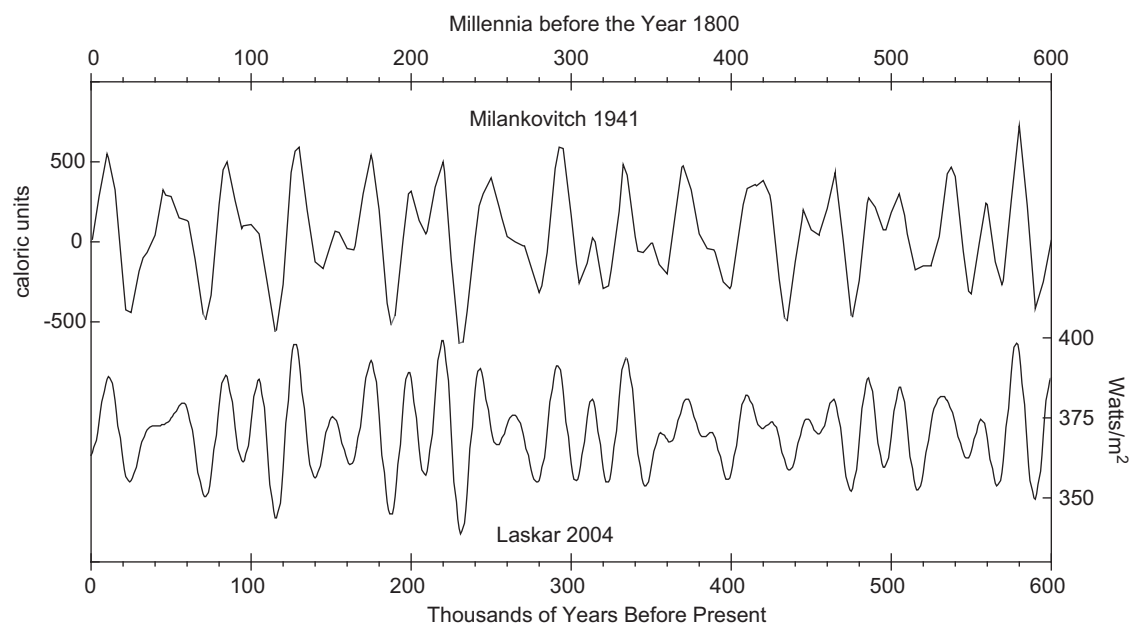
**FIGURE 4.4 The 405-kyr eccentricity metronome.** The nominal La2004 eccentricity series was subjected to Taner bandpass filtering (Taner, 2000) centered at  $1/(405.091 \text{ kyr})$ , with cutoff frequencies set at  $\pm 0.000001 \text{ cycles/kyr}$  on either side of this center frequency. The filtered output was normalized to unity; this constitutes the “single-frequency” 405-kyr metronome. Excerpts are displayed in (a)-(d) (red curve) and illustrate maintenance of phasing through the full La2004 eccentricity solution (black curve) back to 249 Ma (the La2004 model terminus). The number labels indicate 405-kyr cycle number relative to the present. This metronome may be accessed from *TSCreator* (Ogg et al., 2011), which can be downloaded from the website: <http://www.tscreator.com/>. Filtering with cutoff frequencies set at  $\pm 0.001 \text{ cycles/kyr}$  on either side of the center frequency provides a “wide-band” 405-kyr metronome (green curve) for tuning the cyclostratigraphic record from 0–40 Ma with La2004 (0–50 Ma with La2010).

calculations, and the astronomical theory fell into disfavor (review in Imbrie and Imbrie, 1979; update in Broecker and Denton, 1989).

At the same time, significant progress had been made in understanding the origins of the prevalent rhythmic stratification of Mesozoic Alpine limestones (e.g., Schwarzacher, 1947, 1954). This research culminated in the seminal work of Fischer (1964), who found that the meter-scale beds (the so-called Lofer cyclothems) of the Triassic Dachstein Limestone contained vertically repeating facies indicative of shallow marine environments exposed to oscillating sea levels, with

a *ca.* 40 kyr timing. However, glaciations were unknown for the Triassic, raising doubts about the mechanisms by which such sea level oscillations could have occurred; the origin of the Lofer cyclothems continues to be debated today (e.g., Schwarzacher, 1993; Enos and Samankassou, 1998; Cozzi et al., 2005).

It was not until investigation of the Late Quaternary deep-sea sedimentary record that Milankovitch’s theory of climate change was firmly validated. Emiliani (1955, 1966) explained oxygen isotope fractionation in marine calcareous microfauna as a function of ocean temperature and salinity;



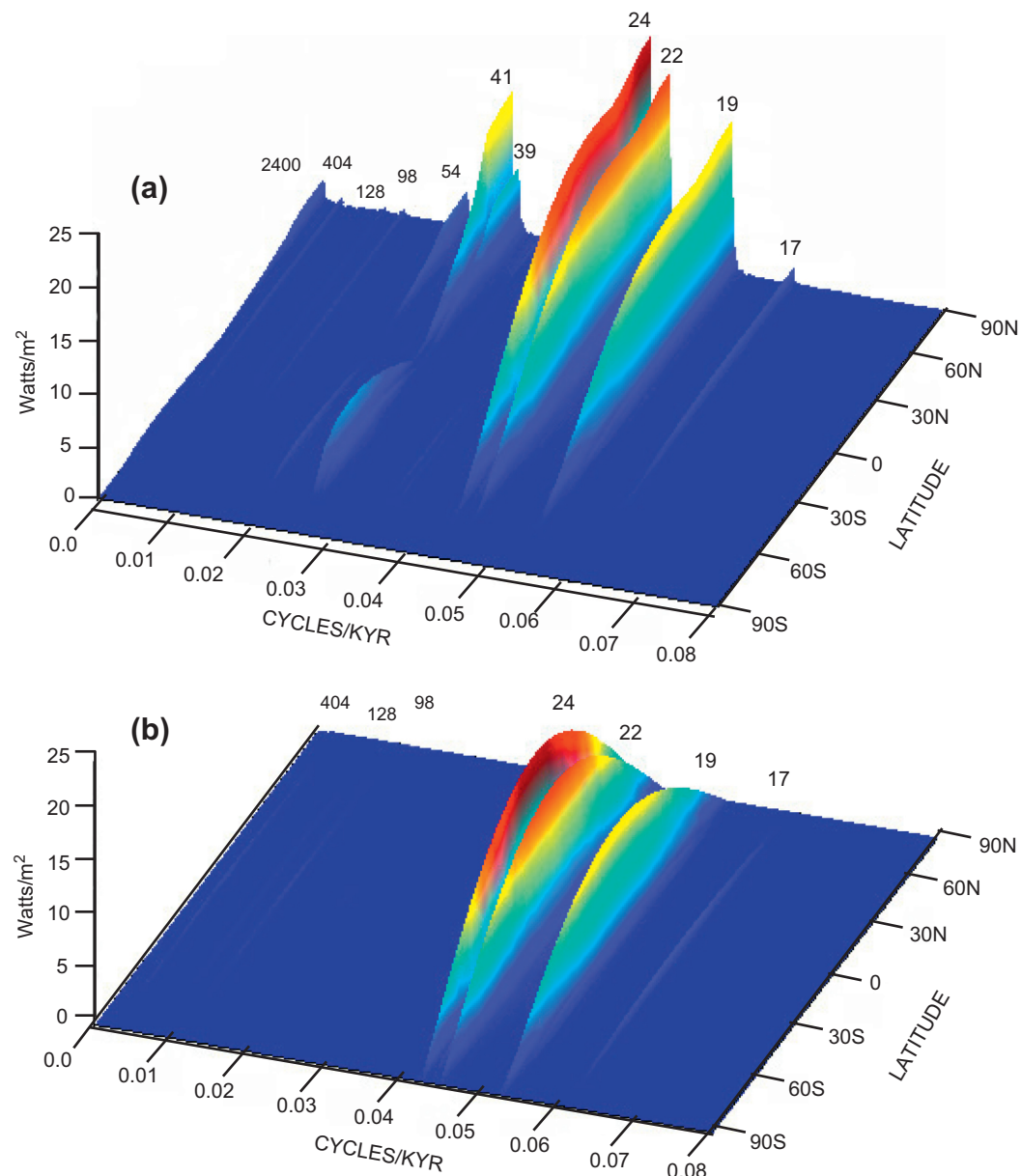
f0030 **FIGURE 4.5** Milankovitch cycles for summer half-year mean insolation at 65° North, 0–600 ka, as originally calculated by Milankovitch (1941; table XXV, p. 513–519) compared with the same calculated with the La2004 nominal model (*Analyseries 2.4.2*).

subsequently, Shackleton (1967) demonstrated that the majority of change in the marine oxygen isotope fractionation was linked to ocean volume (see also Dansgaard and Tauber, 1969). This result was followed by the landmark study of Hays et al. (1976) in which the oxygen isotope record was quantitatively linked to the Milankovitch cycles. Bolstered by the advent of global paleomagnetic stratigraphy in combination with new radioisotopic dates, it was subsequently discovered that the same isotope signal, now encompassing the entire Brunhes chron (0 to 0.78 Ma), was present in all of the major oceans (Imbrie et al., 1984). Finally, calibration of this proxy for global ocean volume to geological evidence for large sea level changes (e.g., Chappell and Shackleton, 1986; Waelbroeck et al., 2002) established, albeit indirectly, the connection between the Quaternary ice ages and Milankovitch cycles. Later research into polar ice stratigraphy uncovered other isotope signals with strong orbital frequencies, providing additional, overwhelming support for the astronomical forcing theory (e.g., Petit et al., 1999; EPICA Community Members, 2004).

p0080 Meanwhile, it was shown convincingly that the astronomical tuning approach, using both oxygen isotopes and sedimentary cycles, could be extended well beyond 800 ka, i.e. the time of the last major glaciations (Shackleton et al., 1990; Hilgen, 1991a, b). These milestone studies touched off multiple initiatives to search for astronomical cycles in stratigraphy back through geologic time, using isotopes as well as other climate proxies, including facies stratigraphy, percent carbonate, biogenic silica, magnetic susceptibility, wireline logs, and grayscale scans (Table 4.1). Continental Pliocene-Pleistocene sediments recovered from Lake Baikal revealed

a strong biogenic silica signal closely mimicking that of the marine isotope record (e.g., Williams et al., 1997; Prokopenko et al., 2006), as do the long Chinese loess sequences (e.g., Sun et al., 2006). Deep sea drilling yielded a continuous oxygen isotope signal spanning 0–6 Ma (Shackleton et al., 1995), and today, there is near-continuous Milankovitch cycle coverage back to the start of the Cenozoic Era from combinations of marine climate proxies from deep sea drilling and outcrop studies (Chapters 28 and 29 of this volume). The Cretaceous/Paleogene boundary was recently the subject of a rigorous intercalibration effort between astrochronology and geochronology (Section 4.8).

Strong evidence for astronomical forcing continues back p0085 into the Mesozoic Era. Multi-million year long cyclostratigraphic successions from all three periods have been tapped for astrochronology and are used in GTS2012 (Chapters 25, 26 and 27). The thick Upper Triassic continental lacustrine deposits of eastern North America contain a nearly perfect eccentricity signal that modulates facies successions linked to wetting-drying climate cycles at precessional time scales. Several of the Mesozoic successions which are now available provide records of continuous astronomical signals that are 20 million years long or more; these include the Aptian-Albian Piobbico core Tethyan sequence (Herbert et al., 1995) and the Carnian-Hettangian Pangean sequence from the Newark Basin Coring Project (Olsen and Kent, 1999), and most recently, the Smithian-Carnian Panthalassic chert sequences of Japan (Ikeda et al., 2010). For geologic times prior to the late Triassic, the evidence for astronomically forced stratigraphy is generally less clear. One reason is that pre-Jurassic oceanic sediments are not composed of the abundant,



f0035 **FIGURE 4.6** Frequency distribution of interannual insolation over 0–5 million years ago, sampled at 1-kyr intervals (*Analyseries*; Paillard et al., 1996) and displayed as multi-tapered amplitude spectra with respect to geographic latitude. (a) Daily mean insolation on June 21 (solstice). Latitudes south of ca. 66°S receive no insolation on this day. Maximum daily insolation occurs in the northern polar regions, which experiences 24-hour exposure. (b) Daily mean insolation on March 21 (equinox). Insolation strength is a function of local solar altitude, highest at the Equator on this day of equal-time exposure everywhere. Contributions from the obliquity variation are absent. [Additional notes: Insolation for the December 21 solstice similar to (a), but with reversed latitudes; and the September 21 equinox is practically identical to (b). Also, the precession component of variation in (a) is at all locations 90° out of phase with the precession component in (b). Additional examples are given in Berger et al., 1993.]

continuous rain of pelagic oozes as are the post-Jurassic ones. Therefore, research is focused more on the prolific shallow marine record, for which the primary evidence of Milankovitch forcing is more a systematic “interruption” rather than a continuous recording (Fischer, 1995).

p0090 Paleozoic formations show clear evidence for astronomical forcing, but none have been integrated into GTS2012. The Permian Castile Formation, a varved marine evaporite

sequence, shows a strong, but short-lived Milankovitch signal (Anderson, 1982, 2010). The spectacular shelf carbonate cycles of the Pennsylvanian Paradox Basin (Utah, USA) indicate high-frequency sea level oscillations with some astronomical signal characteristics (Goldhammer et al., 1994). The classic transgressive-regressive cyclothems of the Pennsylvanian world (e.g., Heckel, 2008) and the rhythmic Mississippian hemipelagic limestones of Ireland



[AU2]  
t0010

**TABLE 4.1**

	Sedimentary Parameter	Associated Climate Conditions
EXTRINSIC (independent of sedimentation rate)	Oxygen isotopes Carbon isotopes Clay assemblages Microfossil assemblages	Temperature/salinity/precipitation/eustasy Productivity/C-sequestration/redox conditions Surface hydrology Salinity/temperature
INTRINSIC (directly related to and/or influenced by sedimentation rate)	Percent CaCO <sub>3</sub> , Si, C <sub>org</sub> Magnetic susceptibility Microfossil abundance Clay/dust abundance Lithofacies Sediment color Grain size	Productivity Sedimentation rate Productivity Surface hydrology/atmospheric circulation Depositional environment Productivity/redox conditions Erosion intensity/hydrodynamics

Commonly measured sedimentary parameters that have been linked to orbitally forced climate change, and the inferred climate conditions. Extrinsic parameters vary independently from sediment supply; intrinsic parameters are directly related to sediment supply, and their signals tend to be more dramatically influenced (distorted) by changes in sedimentation rate (Herbert, 1994).  
Hinnov & Hilgen

(Schwarzacher, 1993) appear to express the dominant 405-kyr eccentricity cycle, conclusions that have recently been supported by high-precision geochronology and cyclostratigraphy of the Donets Basin, Ukraine (Davydov et al., 2010). There are reports of astronomical-scale cycles in Devonian formations (review in Tucker and Garland, 2010), and for the Silurian (e.g., Crick et al., 2001; Nestor et al., 2001, 2003). Stratigraphers have attempted to develop integrated stratigraphy and some astrochronology for the Ordovician (Kim and Lee, 1998; Gong and Droser, 2001; Rodionov et al., 2003) but these efforts remain uncoordinated and largely incomplete. The thick Cambrian-Ordovician cyclic carbonate banks found worldwide show abundant evidence of Milankovitch-scale forcing, although the origins of these high-frequency cyclic sequences remains unsettled (e.g., Osleger, 1995). Research on Cambrian cyclostratigraphy, although off to a productive start several decades ago (e.g., Read, 1995), is presently inactive.

p0095 Precambrian cyclostratigraphy also has evidence for astronomical-like signals. Several shallow marine carbonate successions have been examined, including the meter-scale shallowing upward cycles of the Rocknest Formation, the relict of an early Proterozoic (1.89 Ga) passive margin carbonate platform in the Northwest Territories, Canada (Grotzinger, 1986), and the platform sequence of the late Archean (2.65 Ga) Cheshire Formation, Zimbabwe (Hofmann et al., 2004). However, these records have not been assessed with a specific astronomical model. It has also long been speculated that the banded iron formations (BIFs), with their strong, compound and sustained depositional cyclicality, might have recorded early Milankovitch cycles (e.g., Ito et al., 1993; Hålbich et al., 1993; Simonson and Hassler, 1996). Thus far only one study has attempted to quantify BIF Milankovitch-band cyclicality (Franco and Hinnov, 2008).

#### 4.6. CONSTRUCTING ASTROCHRONOLOGIES AND THE ATS

s0035

The time predictability of the Earth's astronomical parameters invites the practice of using cyclostratigraphy as a high-resolution geochronometer. While this application was already considered by Croll (1867), it was Köppen and Wegener (1924), using insolation curves calculated by Milankovitch, who first calibrated theoretical astronomical-band insolation ("canon of insolation") directly to the geologic record, adjusting approximately known ages of the Late Quaternary Alpine ice ages to the insolation minima of the calculated curves. Significant advances in astrochronology began during the latter half of the 20<sup>th</sup> century with the development of high-resolution global marine oxygen isotope stratigraphy and magnetostratigraphy for the Pleistocene epoch (review in Kent, 1999).

p0100

Absolute astrochronologies recovered from cyclostratigraphy are explicitly connected to the time scale of the astronomical model. For GTS2012, a composite, continuous cyclostratigraphy has provided an absolute astrochronology from the present day back to the Oligocene/Eocene transition (0–34 Ma). Calibration of a cyclostratigraphic sequence begins with the assumption of a target astronomical curve. This may take the form of an insolation signal that most likely affected the climate that influenced sedimentation (e.g., 65°N summer insolation assumed for Pleistocene astrochronology, see Chapter 29), or it can be as simple as the sum of the standardized orbital parameters (e.g., the ETP curve of Imbrie et al., 1984). This assumption introduces a basic uncertainty, because the true nature of the astronomical forcing of the sediment is not known exactly. Hilgen et al. (2000), for example, calibrated Miocene marl-clay deep sea cycles to two possible target curves, 65°N summer insolation and the

p0105

precession index, correlating the mid-points of the marls to the centers of the insolation maxima and precession minima. These two calibrations produced chronologies that differ by several thousand years for any given cycle; this was taken as a fair representation of astrochronologic uncertainty. Other questions persist about which model produces the most accurate astrochronologies back through time related to Earth's tidal dissipation and dynamical ellipticity, which to date have been assessed only in Neogene data (Section 4.7).

p0110 Floating astrochronologies are disconnected from absolute time but are anchored to an independent geochronometer (e.g., a radioisotope-dated horizon, magnetic reversal, or biozone boundary). The astronomical calibration is based upon the assumption that the signal frequencies observed in cyclostratigraphy can be related to one or several frequencies predicted by astronomical modeling, for example, the 405-kyr eccentricity cycle. It is assumed that planetary motions are stable enough to be recognizable back to the geological age represented by the data. This assumption holds reasonably well at least as far back as the Cretaceous/Paleogene boundary (Westerhold et al., 2008, 2009), and there are numerous key similarities between the cyclostratigraphic record and astronomical modeling at times as remote as Triassic (examples in Hinnov and Ogg, 2007).

p0115 The stratigraphic coverage of the ATS that has been assembled for GTS2012 is summarized in Figure 4.7. Considerable progress has been made in the Cenozoic ATS since GTS2004. Astrochronology for the interval between 10–12 Ma that had been based on the continental Orera section in Spain is now replaced by the deep marine Monte dei Corvi section (Hüsing et al., 2007). The downward extension of Monte dei Corvi near La Vedova is used for the interval between 13.5–14.3 Ma (Hüsing et al., 2010; Mourik et al., 2010). Unfortunately, magnetization in the interval between 12–13.5 Ma is too weak, and reversal ages still have to be calculated from marine anomaly profiles. The same is true for the interval 16–23 Ma, but high-resolution studies of ODP sites from Leg 208 (Walvis Ridge; Liebrand et al., 2011) and IODP Leg 320 (equatorial Pacific) offer bright prospects for solving the remaining problems in the Early Miocene ATS, including that of the Oligocene-Miocene boundary, because the cores have reliable magnetostratigraphic records.

p0120 The tuning of the Eocene-Oligocene boundary interval has also improved, in large part from analysis of the Eocene-Oligocene boundary section at Massignano in Italy (e.g., Brown et al., 2009). Part of the Middle Eocene has also been tuned using the classical Contessa section (Jovane et al., 2010). Finally, much progress has been made in constructing an ATS for the entire Paleocene and Early Eocene (Lourens et al., 2005; Westerhold et al., 2007, 2008; Westerhold and Röhl, 2009; Hilgen et al., 2010). This has used the intercalibration of  $^{40}\text{Ar}/^{39}\text{Ar}$  radioisotope dating and astronomical tuning to constrain a first-order tuning (Kuiper et al., 2008). In principle, astronomical tuning prior to 40–50 Ma can only be

carried out at the 405-kyr eccentricity scale in view of limitations in the accuracy of the astronomical solution (Section 4.7). Uncertainties still exist in the number of 405-kyr eccentricity-related cycles in the Paleocene, and several tuning options have been presented that reflect the uncertainty (Westerhold et al., 2008; Hilgen et al., 2010). These problems will likely be resolved in the coming years when high-precision state-of-the-art single crystal  $^{40}\text{Ar}/^{39}\text{Ar}$  sanidine and U-Pb zircon ages become available from key stratigraphic levels such as the Cretaceous-Paleogene, Paleogene-Eocene and Eocene-Oligocene boundaries.

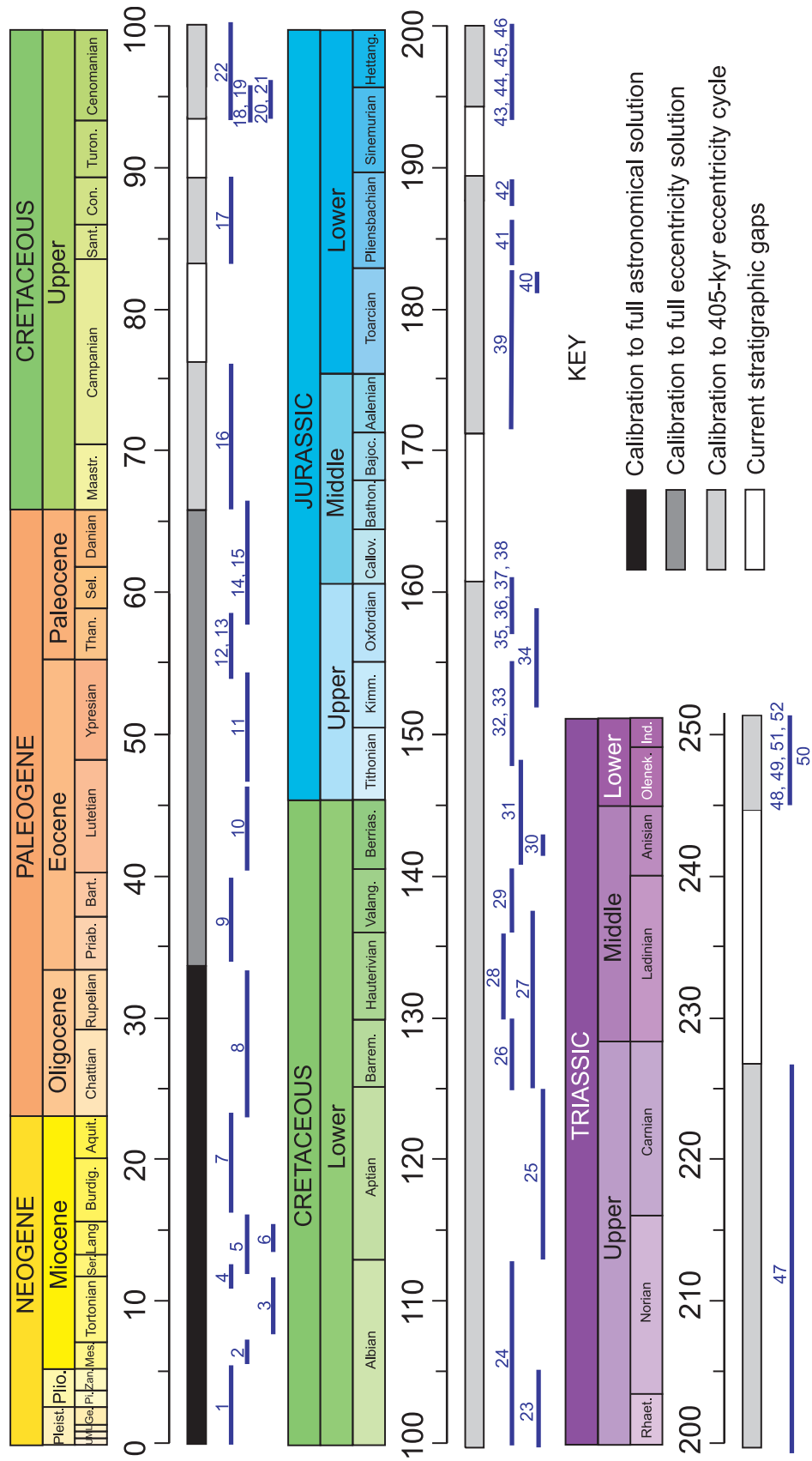
The ATS has been extended, in “floating” form, into the Mesozoic Era, spanning more than 75 percent of the Mesozoic time scale (Figure 4.7). The entire Maastrichtian has now been tuned (Husson et al., 2011); two options are presented, reflecting the ongoing uncertainty in the initial tuning to the orbital eccentricity. Aside from longstanding gaps in the lower Campanian and Turonian, there is continuous stratigraphic coverage to the base of the Oxfordian. Bajocian-Bathonian cyclostratigraphic analysis is ongoing (Ziółkowski and Hinnov, 2010); the Callovian and Sinemurian stages are the only gaps remaining in the Jurassic ATS. The Triassic ATS continues to be dominated by the continental Newark series record (Olsen and Kent, 1996). The Lower Triassic of the Germanic Basin has now been analyzed by several groups (e.g., Bachmann and Kozur, 2004; Menning et al., 2005); the Middle Triassic remains unresolved, in part due to the “Latemar controversy” (Tanner, 2010).

#### 4.7. PRECISION AND ACCURACY OF THE ATS s0040

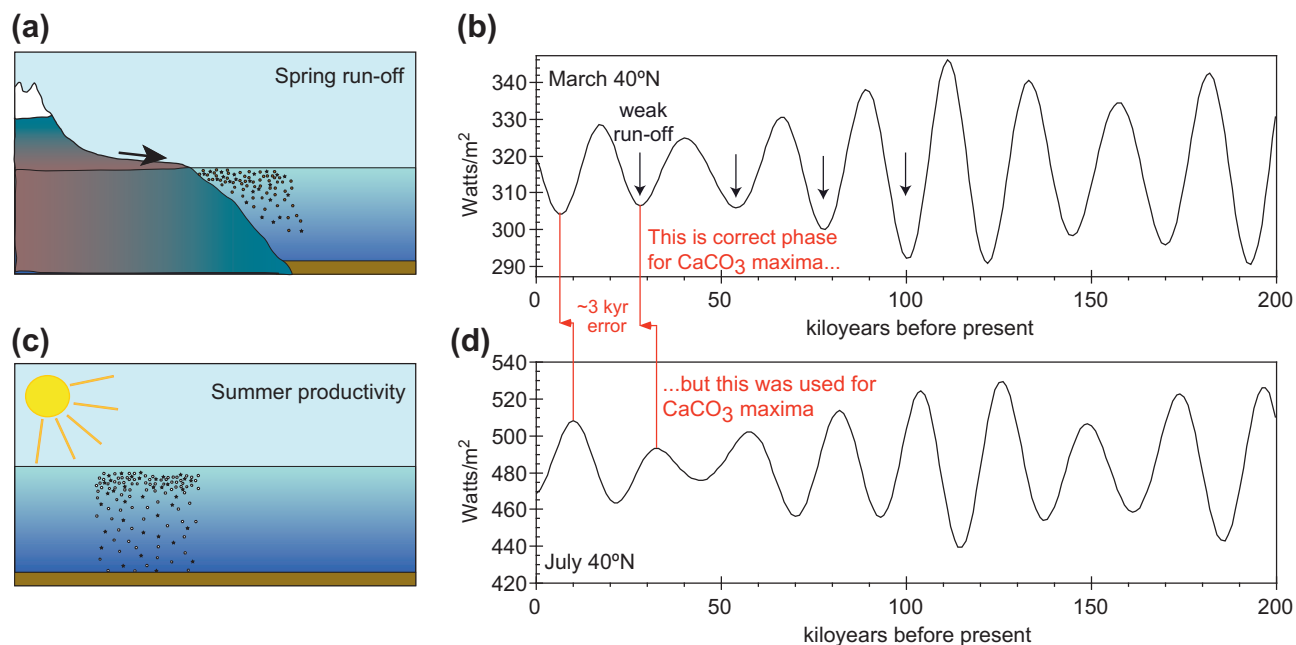
A number of significant factors have been identified that limit the precision and accuracy of the ATS. There are uncertainties in the climatic forcing leading to any given cyclostratigraphic record, and of the geophysical effects on the past precession of the Earth, and in modeling Solar System diffusion prior to 40–50 Ma, as follows.

##### 4.7.1. Seasonal Phase Relations s0045

Tuning to the wrong insolation target curve can result in tuning errors of up to 10–12 kyr (half a precession cycle). For example, consider a marine sedimentary system that experiences depositional cyclicity as the result of dilution of pelagic carbonate from terrestrial run-off that peaks annually in early spring (month of March) (Figure 4.8a); when insolation is low, terrestrial run-off is correspondingly low, and pelagic carbonate deposition is relatively high (Figure 4.8b). Thus, tuning should match insolation minima with carbonate maxima. Suppose that in error it is assumed that peak summer-time ocean productivity was the cause of the pelagic carbonate cyclicity (Figure 4.8c), and that a mid-summer (month of July) insolation target is used to match carbonate



f0040 **FIGURE 4.7** Stratigraphic coverage of the ATS in GTS2012. 1—Lourens et al. (2004); 2—Hilgen et al. (2007); 3—Hüsing et al. (2009); 4—Hilgen et al. (2003); 5—Holburn et al. (2007); 6—Hüsing et al. (2010); 7—Billups et al. (2004); 8—Pälike et al. (2006); 9—Pälike et al. (2001); 10—Jovane et al. (2010); 11—Westerhold and Röhl (2009); 12—Lourens et al. (2005); 13—Westerhold et al. (2007); 14—Westerhold et al. (2008); 15—Kuiper et al. (2008); 16—Husson et al. (2011); 17—Locklair and Sageman (2008); 18—Siewert et al. (2011); 19—Meyers et al. (in press); 20—Meyers et al. (2001); 21—Mitchell et al. (2008); 22—Lanci et al. (2010); 23—Gale et al. (1999); 24—Gale et al. (2011); 25—Grippio et al. (2004); 26—Huang et al. (2010a); 27—Fiet and Gorin (2000); 28—Sprovieri et al. (2006); 29—Huang et al. (1993); 30—Giraud et al. (1995); 31—Spronger and Ten Kate (1993); 32—Huang et al. (2010b); 33—Weedon et al. (2004); 34—Huang et al. (2010c); 35—Strasser (2007); 36—Boullia et al. (2008a); 37—Boullia et al. (2010a); 38—Boullia et al. (2010b); 39—Boullia et al. (2010c); 40—Hinnov and Park (1999); 41—Suan et al. (2008); 42—Huret (2006); 43—Weedon and Jenkyns (1999); 44—Weedon et al. (1999); 45—Kent and Olsen (2008); 46—Ruhl et al. (2010); 47—Whiteside et al. (2010); 48—Olsen and Kent (1996); 49—Bachmann and Kozur (2004); 50—Kozur and Bachmann (2005); 51—Menning et al. (2005); 52—Szuriles (2004); 53—Szuriles (2007).



f0045 **FIGURE 4.8** Example of seasonal uncertainty in astrochronology. (a) A northern mid-latitude marine depositional system in which the source of sedimentary (carbonate-noncarbonate) cyclicity is dilution of pelagic carbonate by terrestrial-derived siliciclastics during early spring (month of March) melt season. (b) The spring run-off depicted in (a) varies with March insolation, such that low insolation corresponds to decreased run-off, hence to pelagic carbonate maxima in the interannual stratigraphic record. (c) An incorrect model in which marine productivity during the summer (month of July) is the source of sedimentary cyclicity. (d) The model in (c) would be assumed to vary with July insolation, such that high insolation corresponds to higher productivity, and to carbonate maxima in the stratigraphic record. In sum, assuming (a)–(b) would result in an accurate tuning of stratigraphy to a March insolation target curve; assuming (c)–(d) would introduce a systematic ~3 kyr error in the tuning, due to an incorrect description of the sedimentary system response to climate change.

maxima to insolation maxima (Figure 4.8d). This results in a systematic error in chronology that is on the order of ~3 kyr. In sum, if very little to nothing is understood about the conditions of sedimentary deposition relative to the local seasonal climate, the seasonal uncertainty can be as large as  $\pm 10$ –12 kyrs (half a precession cycle).

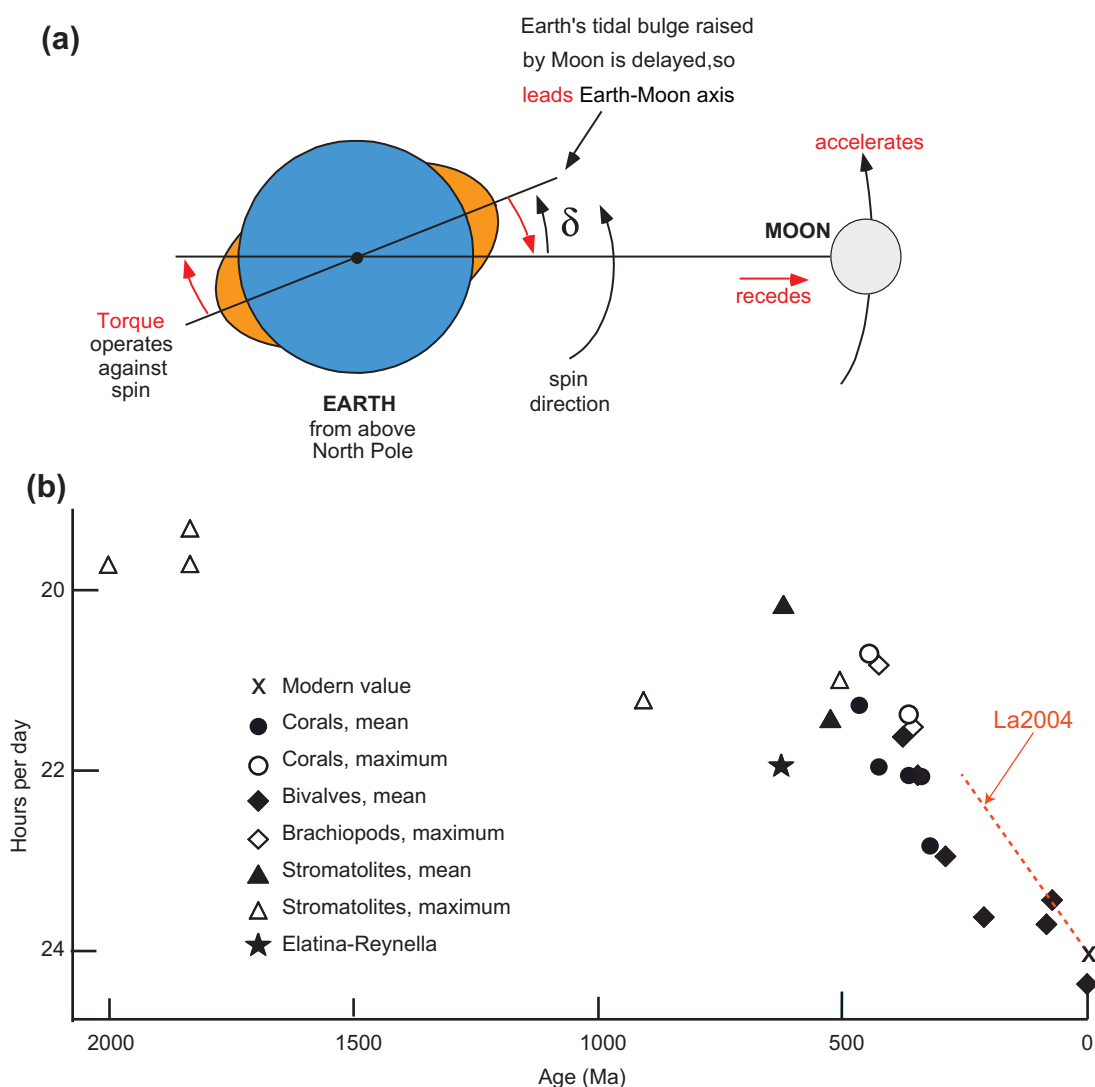
#### s0050 4.7.2. Tidal Dissipation, Dynamical Ellipticity and Climate Friction

p0140 Through geologic time, the Earth's rotation rate has progressively decelerated as a result of tidal energy dissipation. Tidal dissipation results in an exchange of angular momentum between the Earth and Moon, a decreasing Earth rotation, increasing Earth–Moon distance, and lunar recession (Figure 4.9a). Lunar laser ranging from August, 1969 – December, 1993 indicates a lunar recession rate of 3.82 cm/yr, which corresponds to a change in length-of-day of 2.3 ms/century. Geological data confirm that Earth's rotation was faster in the geological past, with apparently a 19-hour length-of-day 1 billion years ago (Figure 4.9b). Changes in rotation rate have not been uniform through time, with greater deceleration occurring after 500 Ma.

p0145 The rotational deceleration increases the Earth's precession rate  $p$ , and in turn, the obliquity and precession periods

(Berger et al., 1992; Laskar et al., 1993a; Ito et al., 1993; Berger and Loutre, 1994). Table 4.2 shows the principal obliquity and precession periods over the past 250 Ma according to the La2004 nominal model, which assumes a length-of-day evolution of 2.68 ms/century, close to the 2.3 ms/century measured by lunar laser ranging (Dickey et al., 1994). In addition, Earth's shape, or dynamical ellipticity, also contributes to  $p$ .

Several pioneering studies have assessed Earth's decel- p0150-  
eration from the cyclostratigraphic record. Lourens et al. (1996) compared astronomical models with different tidal dissipation and dynamical ellipticity values to cyclostratigraphic (oxygen isotope) data from the Mediterranean, Atlantic and Pacific oceans, concluding that the best fit was to a model based on present-day values of dynamical ellipticity and tidal dissipation. Likewise, Pälike and Shackleton (2000) showed that present-day dynamical ellipticity and tidal dissipation applied to astronomical tuning target curves for the past 23 million years produced the best fit with ODP Leg 154 (Ceara Rise) cyclostratigraphy based on magnetic susceptibility. However, in a study of an extremely high-resolution cyclostratigraphic series from 2.4–2.9 Ma, Lourens et al. (2001) found that half of present-day tidal dissipation produced an astronomical model with the best fit. As the global cyclostratigraphic database improves and extends further back in geologic time, renewed investigation



f0050 **FIGURE 4.9 Earth rotation deceleration from tidal energy dissipation.** (a) The Moon raises a tidal bulge that is delayed due to friction between the oceans and crust, and within the solid Earth, by an angle  $\delta$ , which is  $0.2^\circ$  for the solid  $M_2$  tide and  $\sim 65^\circ$  for the net ocean  $M_2$  tide (Munk, 1997; Ray et al., 2001). Gravitational force from the Moon acts on the offset bulge, producing a torque on the Earth in a direction opposite from the rotation, causing the Earth to decelerate. (b) Deceleration of the Earth over the past 2 billion years based on geological data. The data shown are from Williams (2000). Corals, bivalves and brachiopods secrete daily growth bands that modulate annually; fossils indicate more growth bands per year back in time. Stromatolite laminations have been interpreted similarly. Tidalites are an alternate, relatively rare source of information. The red dashed line indicates the length-of-day model used in the nominal La2004 solution of Laskar et al. (2004), which assumes present-day tidal dissipation and dynamical ellipticity. Table 4.2 lists obliquity and precession periodicities for key geological times.

should clarify the long-term evolution of Earth's tidal dissipation and dynamical ellipticity, which are thought to change as a function of continent/ocean configuration, core-mantle processes and crustal loading (e.g., ice sheets).

p0155 Glacial loading of the Earth's crust, i.e., climate friction, is thought to engender "obliquity-oblateness feedback" and secular change in Earth's obliquity (tilt) angle (Bills, 1994; Rubincam, 1995; Ito et al., 1995; Levrard and Laskar, 2003). Thomson (1990) noticed systematic differences between the spectral lines of the Pleistocene SPECMAP stack (Imbrie et al., 1984) and those of the astronomical parameters, suggesting that the recorded signal was perturbed as a result of

the repeated massive ice sheet loading/unloading in the Northern Hemisphere. Thomson discovered a differential phasing in the obliquity and precession bands of SPECMAP that could be explained by varying the precession rate  $p$  by  $\pm 10\%$  at 100,000-year timescales (the scale of the glaciations). Laskar et al. (1993a, b) point out that such a change could allow for passage of  $p$  into resonance with the  $s_6 - g_6 + g_5$  precession term and induce a  $\sim 0.5^\circ$  increase in maximum obliquity. Modeling shows that predicted longer length-of-day in the near future will force precession into this resonance (see Figure 14 in Laskar et al., 2004). However, thus far, no evidence has been presented that Earth's

[AU3]  
t0015

**TABLE 4.2**

(a)					
Time (Ma)	54 kyr	41 kyr	39 kyr	29 kyr	28 kyr
0–5	53562	40917	39510	29727	28852
50–55	50710	39185	37975	28877	28003
100–105	47847	38865	36324	27910	27137
150–155	45188	35852	34807	27027	26233
200–205	42680	34211	33300	26130	25374
244–249	40502	32830	31949	25272	24582
(b)					
Time (Ma)	24 kyr	22 kyr	19.0 kyr	18.9 kyr	16.5 kyr
0–5	23657	22336	19080	18947	16453
50–55	23052	21820	18716	18539	16168
100–105	22472	21304	18335	18090	15873
150–155	21863	20768	18077	17794	15574
200–205	21258	20206	17519	17391	15253
244–249	20691	19708	17129	17007	14968

Dissipation-induced changes in the main periods of the Earth's obliquity variation (a) and precession index (b) from 0 to 250 million years ago. Periods are estimated over 5 million year intervals of the La2004 nominal solution (Laskar et al., 2004) with  $4\pi$  multi-taper amplitude spectra using *Analyseries* (Paillard et al., 1996); values are in thousands of years. Hinnov & Hilgen

precession has undergone resonance as the result of climate friction.

### s0055 4.7.3. Solar System Diffusion

p0160 Modeling experiments demonstrate that the inner planets of the Solar System experienced significant chaotic diffusion throughout the remote past (Laskar 1990; Laskar et al., 1992; Laskar, 1994). Over the past ~40 million years, the Earth and Mars orbits have been in 2:1 secular resonance, described by the argument  $\theta = (s_4 - s_3) - 2(g_4 - g_3)$ , where  $s_3$  and  $s_4$  are secular frequencies defining the rotation of the ascending nodes of the orbits, and  $g_3$  and  $g_4$  are secular frequencies for the rotation of orbital perihelia of Earth and Mars (Matthews et al., 1997; Laskar, 1999; Laskar et al., 2004). Prior to 40 million years ago, modeling indicates that the two orbits experienced intermittent chaotic transitions, and 1:1 resonance states, i.e.,  $\theta = (s_4 - s_3) - (g_4 - g_3)$  (e.g., Figure 23 in Laskar et al., 2004). These resonance states may be observed indirectly in paleoclimate data in long-period modulations of Earth's obliquity and precession index, in the beat frequencies produced by the terms  $p + s_3$  (1/41 kyr) and  $p + s_4$  (1/39 kyr) in

the obliquity, and  $p + g_3$  (1/19.1 kyr) and  $p + g_4$  (1/18.9 kyr) in the precession index, where  $p = 50.4467718''/\text{yr}$  is the Earth precession rate (variable through time due to tidal dissipation and dynamical ellipticity). The term  $g_4 - g_3$  is also present in Earth's orbital eccentricity as a long-period modulation in the ~100 kyr variation, e.g., the beat frequency raised by  $g_4 - g_5$  (1/94.9 kyr) and  $g_3 - g_5$  (1/98.8 kyr).

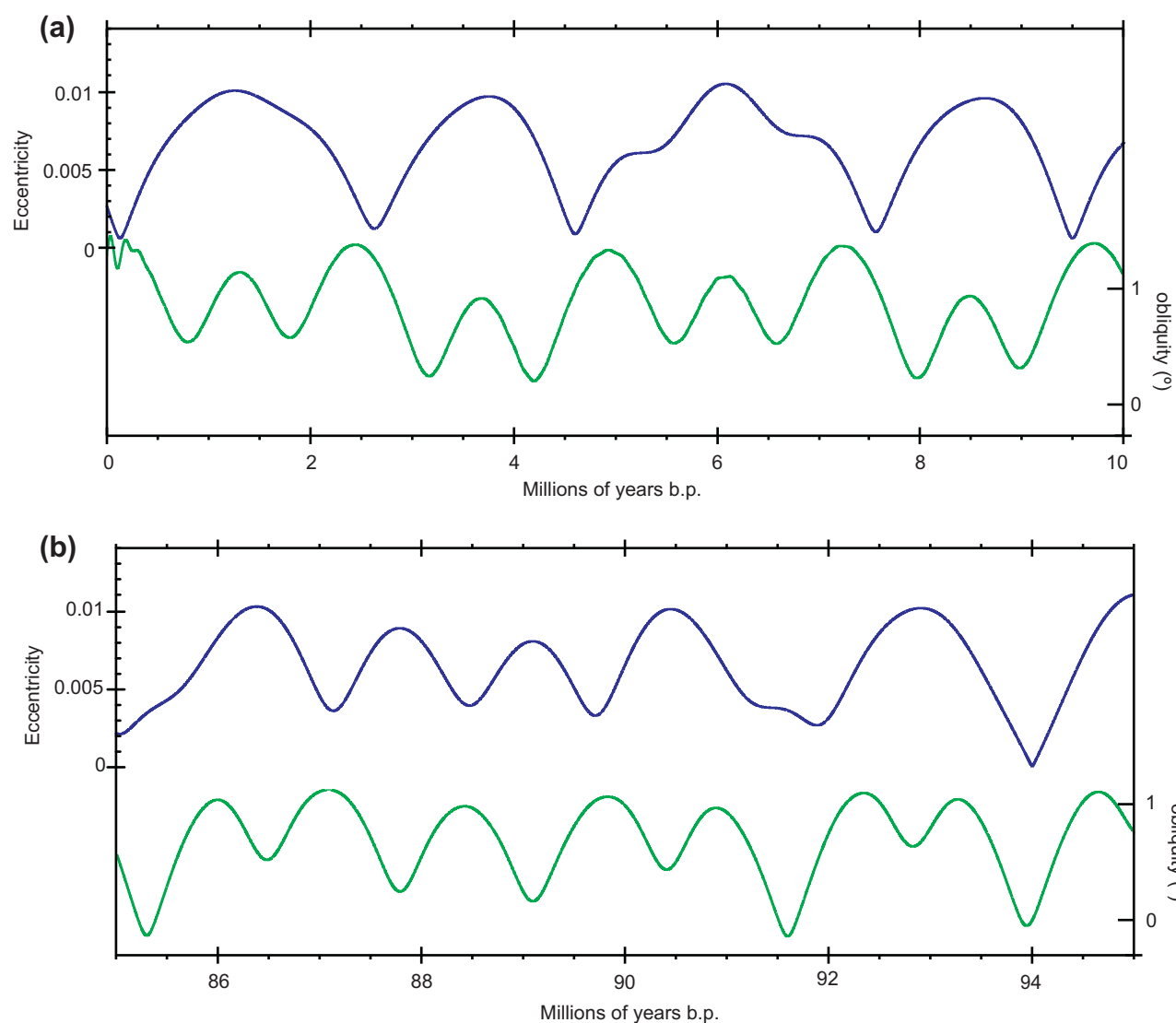
Figure 4.10 shows  $s_4 - s_3$  and  $g_4 - g_3$  in the modulation envelopes of the La2004 obliquity and eccentricity, for which the former has a ~1.2 myr periodicity, and the latter, a ~2.4 myr periodicity, over 0–10 Ma; also shown are the modulations over 85–95 Ma to illustrate transient shortening of the modulations from chaotic diffusion. These modulations have been confirmed in Cenozoic stratigraphy, notably across the Miocene-Oligocene transition in deep-sea sedimentary sequences recovered by the Ocean Drilling Program (Shackleton et al., 1999; Pälike et al., 2004). In the future, the documentation of Earth-Mars secular resonance states throughout the Mesozoic Era will provide key constraints on the gravitational parameters used in Solar System modeling (Laskar 2003; Laskar et al., 2004).

### 4.7.4. Summary of Uncertainties

In Figure 4.11 the “tidal uncertainty” refers to lack of knowledge about Earth's past tidal dissipation and its effect on the precession rate, which presents as an accumulating deficit of years in the recorded obliquity and precession cycles back through time (Figure 20.7 in Lourens et al., 2004). As this amount accumulates, at some point it becomes necessary to tune instead to the orbital eccentricity; this is depicted at 50 Ma. At times prior to 50 Ma, astronomical models diverge as the combined result of initial condition uncertainties and integration error, with close agreement only for the 405-kyr eccentricity cycle back to 250 Ma. Sometime between 50 and 100 Ma, modeling indicates that a “transition” occurred in the resonance state between the Earth and Mars orbits, which would have affected the 100-kyr eccentricity variation. This is shown by the shaded area labeled “transition”, at which point it becomes necessary to restrict tuning to the 405-kyr cycle only. The precise timing of the transition will be determined through future, detailed examination of the cyclostratigraphic record (Laskar et al., 2011).

## 4.8. ASTROCHRONOLOGY-GEOCHRONOLOGY INTERCALIBRATION

The extension of the astronomical dating method into the Middle–Early Pleistocene and Pliocene (Shackleton et al., 1990; Hilgen, 1991a, b) stimulated much research directed at the comparison of astronomical and radio-isotopic ages, especially because astronomical ages proved to be significantly older – by ~3 to 12% – than published K/Ar ages for the same magnetic reversal boundaries. This discrepancy was

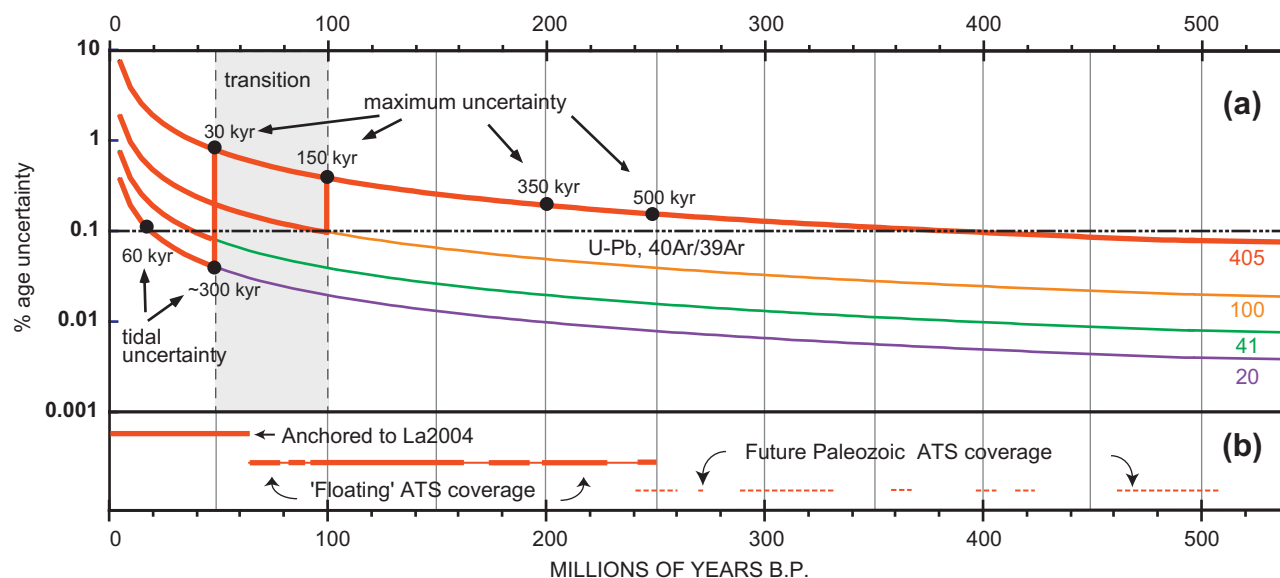


f0055 **FIGURE 4.10** Amplitude modulations (AM) of the eccentricity (blue lines) and obliquity (green lines). The eccentricity modulations have a dominant  $\sim 2.45$  myr periodicity, and the obliquity modulations have a 1.2 myr periodicity. These AM curves were estimated by applying Hilbert transforms to Taner bandpass filtered (Taner, 2000) La2004 eccentricity and obliquity series over 0–249 Ma with a passband of  $0.01025 \pm 0.00075$  cycles/kyr (short eccentricity) and a passband of  $0.0275 \pm 0.0045$  cycles/kyr (main obliquity). The filtered series were Hilbert-transformed (Taner et al., 1979) to obtain the amplitude modulations. The two excerpts illustrate (a) 2:1 secular resonance from 0–10 Ma, and (b) 1:1 resonance indicated by the frequency correspondence between eccentricity and obliquity from 87–90 Ma.

largely attributed to incomplete Ar degassing of basaltic bulk rock samples used for dating the reversals (Hilgen et al., 1991b). The switch to  $^{40}\text{Ar}/^{39}\text{Ar}$  dating led to very accurate and precise ages, but only the analytical error, leading in K/Ar dating, was initially taken into account and not the full error of  $\sim 2.5\%$  that included such factors as uncertainties in the decay constants and mineral dating standards (Min et al., 2000). This encouraged further research, as the error in astronomical dating is comparatively small once the tuning itself is correct ( $\sim 0.1\%$  between 5 and 10 Ma; e.g. Kuiper et al., 2008).

p0180 [AU1] Following earlier attempts (e.g., Renne et al., 1994; Hilgen et al., 1997), a direct intercalibration was achieved

through a direct comparison of astronomical and Ar/Ar ages of ash beds intercalated in astronomically tuned marine sections in the Melilla Basin in Morocco (Kuiper et al., 2008). This study revealed a systematic offset with astronomical ages being  $\sim 0.7\%$  older. This offset was removed by fitting the  $^{40}\text{Ar}/^{39}\text{Ar}$  ages to the astronomical ages by adjusting the age of the Fish Canyon tuff sanidine (FCs) dating standard from  $28.02 \pm 0.28$  Ma (Renne et al., 1998) to  $28.201 \pm 0.046$  Ma. Consequently, the error in the astronomically calibrated FCs age is greatly reduced due to the fact that uncertainties related to decay constants and the age of the primary dating standard which together



f0060 **FIGURE 4.11** Summary of current ATS uncertainty and stratigraphic coverage through the Phanerozoic Eon. (a) Lower limit of age uncertainty (in %) from high-precision geochronology (dash-dot line) and cyclostratigraphy (solid curves). Red lines indicate the geologic time intervals for which the different modeled astronomical parameters may be used with confidence. “Tidal uncertainty” refers to the uncertainty in knowledge of past tidal friction and its effect on the Earth’s rotation and precession rate  $p$  (Lourens et al., 2004). “Maximum uncertainty” on the 405-kyr term refers to uncertainty estimated from differences among six different astronomical models (Laskar et al., 2004). The shaded area labeled “transition” refers to the latest predicted Earth-Mars orbital resonance transition. The 405-kyr orbital eccentricity term prior to 250 Ma has not been modeled, and so maximum uncertainty has not been extended into the Paleozoic Era. (b) Stratigraphic coverage of the ATS in GTS2012 in solid red lines; future ATS coverage for the Paleozoic Era (potential candidates in Section 4.5) in dashed red lines. The Cenozoic ATS is anchored to the La2004 solution, although uncertainties persist in Paleogene tuning. The Mesozoic ATS is a “floating” timescale, anchored locally by radioisotope dating, but not to a specific astronomical solution.

dominate the full error in  $^{40}\text{Ar}/^{39}\text{Ar}$  dating are effectively eliminated.

p0185 The  $28.201 \pm 0.046$  Ma FCs age has been independently confirmed by  $^{40}\text{Ar}/^{39}\text{Ar}$  dating of the A1 ashbed in the astronomically tuned Faneromeni section, and U-Pb dating of single zircon crystals in the Fish Canyon tuff and in ash beds from the astronomically dated Monte dei Corvi section (Rivera et al., in press; Wotzlaw et al., 2010). These results suggest that the FCs age of 28.30 Ma based on  $^{40}\text{Ar}/^{39}\text{Ar}$ -U-Pb pairs and neglecting astronomical dating (Renne et al., 2010) is too old, and that an FCs age of 27.93 Ma based on  $^{40}\text{Ar}/^{39}\text{Ar}$ -astrochronologic intercalibration of the Matayuma/Brunhes transition (Channell et al., 2010) is too young. The  $28.201 \pm 0.046$  Ma FCs standard is further supported by a three-way intercalibration of  $^{40}\text{Ar}/^{39}\text{Ar}$ , U-Pb and astrochronology across the Cenomanian/Turonian boundary (Meyers et al., in press), and by a direct comparison of U/Pb and  $^{40}\text{Ar}/^{39}\text{Ar}$  ages of two ash beds from the Eocene Green River Formation, allowing a direct comparison with the astronomical solution for the first time (Smith et al., 2010). The intercalibration guarantees that astronomical and  $^{40}\text{Ar}/^{39}\text{Ar}$  dating will produce the same age when the same event in Earth history is dated. The astronomically calibrated FCs standard provides unprecedented tight constraints for the tuning of pre-Neogene successions. In this way, problems such as the existing Eocene gap in the ATS or the reduced

reliability of the astronomical solution further back in time can be circumvented.

#### 4.9. A NEW ASTRONOMICAL SOLUTION

A new solution, La2010, has now been made available (Laskar et al., 2011). This solution is limited to the orbital eccentricity, and uses the new, highly accurate ephemeris solution INPOP10 over short time scales (Fienga et al., 2009, 2010). La2010 is reliable back to 50 Ma, as compared to 40 Ma for La2004. This is a major improvement, as the solution must be one order more accurate in order to extend its reliability by an additional 10 myr (Laskar et al., 2004). La2010 will play a major role in solving problems presently encountered in the tuning of the Paleocene and early Eocene (Westerhold et al., 2008; Hilgen et al., 2010). It will shed light on the possibility of long-period eccentricity forcing of Eocene hyperthermals (Lourens et al., 2005) and Mesozoic black shales (Mitchell et al., 2008).

#### REFERENCES

- Adhémar, J., 1842. Les révolutions de la mer, déluges périodiques. Carilian-Gouery et V. Dalmort, Paris, p. 184.  
 Anderson, R.Y., 1982. A long geoclimatic record from the Permian. *Journal of Geophysical Research* 87, 7285–7294.

s0070  
p0190

cesectitle00



- Anderson, R.Y., 2010. Earth as diode: monsoon source of the orbital ~100 ka climate cycle. *Climate of the Past Discussions* 6, 1421–1452.
- Bachmann, G.H., Kozur, H.W., 2004. The Germanic Triassic: correlations with the international chronostratigraphic scale, numerical ages and Milankovitch cyclicity. *Hallesches Jahrbuch für Geowissenschaften* B26, 17–62.
- Berger, A., Loutre, M.-F., 1994. Astronomical forcing through geologic time. In: DeBoer, P., Smith, D.G. (Eds.), *Orbital Forcing and Cyclic Sequences*. International Association of Sedimentologists, Special Publication, 19, pp. 15–24.
- Berger, A., Loutre, M.-F., Laskar, J., 1992. Stability of the astronomical frequencies over Earth's history for paleoclimate studies. *Science* 255, 560–566.
- Berger, A., Loutre, M.-F., Tricot, C., 1993. Insolation and Earth's orbital periods. *Journal of Geophysical Research* 98, 10341–10362.
- Berger, A., Loutre, M.-F., Yin, Q., 2010. Irradiation during any time interval of the year using elliptic integrals. *Quaternary Science Reviews* 29, 1968–1982.
- Bills, B.G., 1994. Obliquity-oblateness feedback: are climatically sensitive values of obliquity dynamically unstable? *Geophysical Research Letters* 21, 177–180.
- Billups, K., Pälike, H., Channell, J., Zachos, J., Shackleton, N.J., 2004. Astronomic calibration of the Late Oligocene through Early Miocene Geomagnetic Polarity Time Scale. *Earth and Planetary Science Letters* 224, 33–44.
- Bouilila, S., Hinnov, L.A., Collin, P.Y., Huret, E., Galbrun, B., Fortwengler, D., 2008a. Astronomical calibration of the Lower Oxfordian (Terres Noires, Vocontian Basin, France): consequences of revising Late Jurassic time scale. *Earth and Planetary Science Letters* 276, 40–51.
- Bouilila, S., Galbrun, B., Hinnov, L., Collin, P.Y., 2008b. Orbital calibration of the Early Kimmeridgian (Southeastern France): implications for geochronology and astrophysics. *Terra Nova* 20, 455–462.
- Bouilila, S., Galbrun, B., Hinnov, L.A., Collin, P.-Y., Ogg, J.G., Fortwengler, D., Marchand, D., 2010a. Milankovitch and sub-Milankovitch forcing of the Oxfordian (Late Jurassic) Terres Noires Formation (SE France) and global implications. *Basin Research* 22, 717–732.
- Bouilila, S., de Rafélis, M., Hinnov, L.A., Gardin, S., Galbrun, B., Collin, P.-Y., 2010b. Orbitally forced climate and sea-level changes in the Paleoeceanic Tethyan domain (marl-limestone alternations, Lower Kimmeridgian, SE France). *Palaeogeography, Palaeoclimatology, Palaeoecology* 292, 57–70.
- Bradley, W.H., 1929. The varves and climate of the Green River epoch. *US Geological Survey Professional Paper* 158–E, 87–110.
- Broecker, W.S., Denton, G.H., 1989. The role of ocean-atmosphere reorganizations in glacial cycles. *Geochimica et Cosmochimica Acta* 53, 2465–2501.
- Brown, R.E., Koeberl, C., Montanari, A., Bice, D.M., 2009. Evidence for a change in Milankovitch forcing caused by extraterrestrial events at Massignano, Italy. Eocene-Oligocene boundary GSSP. *Geological Special Papers* 452, 119–137.
- Channell, J.E.T., Hodell, D.A., Singer, B.S., Xuan, C., 2010. Reconciling astrochronological and  $^{40}\text{Ar}/^{39}\text{Ar}$  ages for the Matuyama-Brunhes boundary and late Matuyama Chron. *Geochemistry, Geophysics, Geosystems* 11, Q0AA12. doi: 10.1029/2010GC003203.
- Chappell, J., Shackleton, N.J., 1986. Oxygen isotopes and sea level change. *Nature* 324, 137–140.
- Cozzi, A., Hinnov, L.A., Hardie, L.A., 2005. Orbitally forced Lofer cycles in the Dachstein Limestone of the Julian Alps (NE Italy). *Geology* 33, 789–792.
- Crick, R.E., Ellwood, B.B., Hladil, J., El Hassani, A., Hroudra, F., Chlupáč, I., 2001. Magnetostratigraphy susceptibility of the Pridolian-Lochkovian (Silurian-Devonian) GSSP (Klonk, Czech Republic) and a coeval sequence in Anti-Atlas Morocco. *Palaeogeography, Palaeoclimatology, Palaeoecology* 167, 73–100.
- Croll, J., 1867. On the excentricity of the earth's orbit and its physical relations to the glacial epoch. *Philosophical Magazine* 33, 119–131.
- Croll, J., 1875. *Climate and Time in Their Geological Relations*. Appleton, New York, 577 pp.
- Dansgaard, W., Tauber, H., 1969. Glacier oxygen-18 content and Pleistocene ocean temperatures. *Science* 166, 499–502.
- Davydov, V.I., Crowley, J.L., Schmitz, M.D., Poletaev, V., 2010. High-precision U-Pb zircon age calibration of the global Carboniferous time scale and Milankovitch band cyclicity in the Donets Basin, eastern Ukraine. *Geochemistry, Geophysics, Geosystem* 11, Q0AA04. doi:10.1029/2009GC002736.
- Dickey, J.O., Bender, P.L., Faller, J.E., Newhall, X.X., Ricklefs, R.L., Ries, J.G., Shelus, P.J., Veillet, C., Whipple, A.L., Wiant, J.R., Williams, J.G., Yoder, C.F., 1994. Lunar Laser Ranging: a continuing legacy of the Apollo program. *Science* 265, 482–490.
- Emiliani, C., 1955. Pleistocene temperatures. *Journal of Geology* 63, 538–578.
- Emiliani, C., 1966. Isotopic paleotemperatures. *Science* 154, 851–857.
- Enos, P., Samankassou, E., 1998. Lofer cyclothem revisited (Late Triassic, Northern Alps, Austria). *Facies* 38, 207–228.
- EPICA Community Members, 2004. Eight glacial cycles from an Antarctic ice core. *Nature* 429, 623–628.
- Fienga, A., Laskar, J., Morley, T., Manche, H., Kuchynka, P., Le Poncin-Lafitte, C., Budnik, F., Gastineau, M., Somenzi, L., 2009. INPOP08, a 4-D planetary ephemeris: from asteroid and time-scale computations to ESA Mars Express and Venus Express contributions. *Astronomy and Astrophysics* 507, 1675–1686.
- Fienga, A., Manche, H., Kuchynka, P., Laskar, J., Gastineau, M., 2010. INPOP10a. Scientific and Technical Notes of the IMCCE, p. 18. Available from: [www.imcce.fr/inpop/inpop10a.pdf](http://www.imcce.fr/inpop/inpop10a.pdf).
- Fiet, N., Gorin, G., 2000. Lithological expression of Milankovitch cyclicity in carbonate-dominated, pelagic, Barremian deposits in central Italy. *Cretaceous Research* 21, 457–467.
- Fischer, A.G., 1964. Lofer cyclothem of the alpine Trias. *Kansas Geological Survey Bulletin* 14, 351–376.
- Fischer, A.G., 1995. Cyclostratigraphy, Quo Vadis? In: House, M.R., Gale, A.S. (Eds.), *Orbital forcing timescales and cyclostratigraphy*. Geological Society Special Publication, 85, pp. 199–204.
- Franco, D.R., Hinnov, L.A., 2008. Strong rhythmicity in the ~2.46–2.50 Ga banded iron formation of the Hamersley Group (W. Australia): evidence for sub-orbital to Milankovitch scale cycles. Geological Society of America Annual Meeting Houston, TX, 5–9 October, abstract.
- Gale, A.S., Young, J.R., Shackleton, N.J., Crowhurst, S.J., Wray, D.S., 1999. Orbital tuning of Cenomanian marly chalk successions: towards a Milankovitch time-scale for the Late Cretaceous. *Philosophical Transactions of the Royal Society, London, Series A* 357, 1815–1829.
- Gale, A.S., Hardenbol, J., Hathway, B., Kennedy, W.J., Young, J.R., Phansalkar, V., 2002. Global correlation of Cenomanian (Upper Cretaceous) sequences: evidence for Milankovitch control. *Geology* 30, 291–294.
- Gale, A.S., Bown, P., Caron, M., Crampton, J., Crowhurst, S.J., Kennedy, W.J., Petrizzo, M.R., Wray, D.S., 2011. The uppermost Middle and Upper Albian succession at the Col de Palluel, Hautes-

- Alpes, France: an integrated study (ammonites, inoceramid bivalves, planktonic foraminifera, nannofossils, geochemistry, stable oxygen and carbon isotopes, cyclostratigraphy). *Cretaceous Research* 32, 59–130.
- Gilbert, G.K., 1895. Sedimentary measurement of geological time. *Journal of Geology* 3, 121–127.
- Giraud, F., Beaufort, L., Cotillon, P., 1995. Periodicities of carbonate cycles in the Valanginian of the Vocontian Trough: a strong obliquity control. In: House, M.R., Gale, A.S. (Eds.), *Orbital forcing time-scales and cyclostratigraphy*. Geological Society of London Special Publication, 85, pp. 143–164.
- Goldhammer, R.K., Oswald, E.J., Dunn, P.A., 1994. High-frequency, glacio-eustatic cyclicity in the middle Pennsylvanian of the Paradox Basin: an evaluation of Milankovitch forcing. In: deBoer, P.L., Smith, D.G. (Eds.), *Orbital Forcing and Cyclic Sequences*. Special Publication of the International Association of Sedimentologists, 19, pp. 243–283.
- Gong, Y., Droser, M.L., 2001. Periodic anoxic shelf in the Early-Middle Ordovician transition: ichnosedimentologic evidence from west-central Utah, USA. *Science in China, Series D* 44, 979–989.
- Grippo, A., Fischer, A.G., Hinnov, L.A., Herbert, T.D., Premoli Silva, I., 2004. Cyclostratigraphy and chronology of the Albian stage (Piobbico core, Italy). In: D'Argenio, B., Fischer, A.G., Premoli Silva, I., Weissert, H., Ferreri, V. (Eds.), *Cyclostratigraphy: approaches and case histories*. SEPM Special Publication, 81, pp. 57–81.
- Grotzinger, J.P., 1986. Upward shallowing platform cycles: a response to 2.2 billion years of low-amplitude, high-frequency (Milankovitch band) sea level oscillations. *Paleoceanography* 1, 403–416.
- Hälbich, I.W., Scheepers, R., Lamprecht, D., Van Deventer, J.L., De Kock, N.J., 1993. The Transvaal-Griqualand West banded iron formation: geology, genesis, iron exploitation. *Journal of African Earth Sciences* 16, 63–120.
- Hays, J.D., Imbrie, J., Shackleton, N.J., 1976. Variations in the Earth's orbit: pacemaker of the ice ages. *Science* 194, 1121–1132.
- Heckel, P.H., 2008. Pennsylvanian cyclothems in mid-continent North America as far-field effects of waxing and waning of Gondwana ice sheets. *Special Paper of the Geological Society of America* 441, 275–289.
- Herbert, T.D., 1994. Reading orbital signals distorted by sedimentation: models and examples. In: deBoer, P.L., Smith, D.G. (Eds.), *Orbital Forcing and Cyclic Sequences*. Special Publication of the International Association of Sedimentologists, 19, pp. 483–507.
- Herbert, T.D., Premoli Silva, I., Erba, E., Fischer, A.G., 1995. Orbital chronology of Cretaceous-Paleocene marine sediments. In: Berggren, W.A., Kent, D.V., Aubry, M.-P., Hardenbol, J. (Eds.), *Geochronology, time scales and global stratigraphic correlation*. SEPM Special Publication, 54, pp. 81–93.
- Herschel, J.F.W., 1830. On the geological causes which may influence geological phenomena. *Geological Transactions* 3, 293–299.
- Hilgen, F.J., 1991a. Astronomical calibration of Gauss to Matuyama sapropels in the Mediterranean and implication for the Geomagnetic Polarity Time Scale. *Earth and Planetary Science Letters* 104, 226–244.
- Hilgen, F.J., 1991b. Extension of the astronomically calibrated (polarity) time scale to the Miocene-Pliocene boundary. *Earth and Planetary Science Letters* 107, 349–368.
- Hilgen, F.J., 2010. Astronomical tuning in the 19<sup>th</sup> century. *Earth-Science Reviews* 98, 65–80.
- Hilgen, F.J., Krijgsman, W., Langereis, C.G., Lourens, L.J., 1997. Break-through made in dating of the geological record. *Eos* 78, 285–288.
- Hilgen, F.J., Bissoli, L., Iaccarino, S., Krijgsman, W., Meijer, R., Negri, A., Villa, G., 2000. Integrated stratigraphy and astrochronology of the Messinian GSSP at Oued Akrech (Atlantic Morocco). *Earth and Planetary Science Letters* 182, 237–251.
- Hilgen, F.J., Abdul Aziz, H., Krijgsman, W., Raffi, I., Turco, E., 2003. Integrated stratigraphy and astronomical forcing of the Serravallian and lower Tortonian at Monte dei Corvi (Middle-Upper Miocene, northern Italy). *Palaeogeography, Palaeoclimatology, Palaeoecology* 199, 229–264.
- Hilgen, F.J., Kuiper, K., Krijgsman, W., Snel, E., van der Laan, E., 2007. Astronomical tuning as the basis for high resolution chronostratigraphy: the intricate history of the Messinian Salinity Crisis. *Stratigraphy* 4, 231–238.
- Hilgen, F.J., Kuiper, K.F., Lourens, L.J., 2010. Evaluation of the astronomical time scale for the Paleocene and earliest Eocene. *Earth and Planetary Science Letters* 300, 139–151.
- Hinnov, L.A., Park, J., 1999. Strategies for assessing Early-Middle (Pliensbachian-Aalenian) Jurassic cyclochronologies. In: Shackleton, N.J., McCave, I.N., Weedon, G.P. (Eds.), *A Discussion: Astronomical (Milankovitch) Calibration of the Geological Timescale*. Philosophical Transactions of the Royal Society, London, Series A, 357, pp. 1831–1859.
- Hinnov, L.A., Ogg, J.G., 2007. Cyclostratigraphy and the Astronomical Time Scale. *Stratigraphy* 4, 239–251.
- Hofmann, A., Dirks, P.H.G.M., Jelsma, H.A., 2004. Shallowing upward carbonate cycles in the Belingwe Greenstone Belt, Zimbabwe: a record of Archean sea-level oscillations. *Journal of Sedimentary Research* 74, 64–81.
- Holbourn, A., Kuhnt, W., Schulz, M., Flores, J.-A., Andersen, N., 2007. Orbitally-paced climate evolution during the middle Miocene “Monterey” carbon-isotope excursion. *Earth and Planetary Science Letters* 261, 534–550.
- Huang, Z., Ogg, J.G., Gradstein, F.M., 1993. A quantitative study of Lower Cretaceous cyclic sequences from the Atlantic Ocean and Vocontian Basin (SE France). *Paleoceanography* 8, 275–291.
- Huang, C., Hinnov, L.A., Fischer, A.G., Grippo, A., Herbert, T., 2010a. Astronomical tuning of the Aptian stage from Italian reference sections. *Geology* 38, 899–903.
- Huang, C., Hinnov, L.A., Swientek, O., Smelner, M., 2010b. Astronomical tuning of Late Jurassic-early Cretaceous sediments (Volgian-Ryazanian stages), Greenland-Norwegian Seaway. *American Association of Petroleum Geologists Annual Convention New Orleans, LA, 11–14 April, 2010*, abstract.
- Huang, C., Hesselbo, S.P., Hinnov, L.A., 2010c. Astrochronology of the Late Jurassic Kimmeridge Clay (Dorset, England) and implications for Earth system processes. *Earth and Planetary Science Letters* 289, 242–255.
- Hüsing, S.K., Hilgen, F.J., Abdul Aziz, H., Krijgsman, W., 2007. Completing the Neogene geological time scale between 8.5 and 12.5 Ma. *Earth and Planetary Science Letters* 253, 340–358.
- Hüsing, S.K., Kuiper, K.F., Link, W., Hilgen, F.J., Krijgsman, W., 2009. The upper Tortonian-lower Messinian at Monte dei Corvi (Northern Italy): completing a Mediterranean reference section for the Tortonian Stage. *Earth and Planetary Science Letters* 282, 140–157.
- Hüsing, S.K., Cascella, A., Hilgen, F.J., Krijgsman, W., Kuiper, K.F., Turco, E., Wilson, D., 2010. Astrochronology of the Mediterranean Langhian between 15.29 and 14.17 Ma. *Earth and Planetary Science Letters* 290, 254–269.
- Huret, E., 2006. Analyse cyclostratigraphique des variations de la susceptibilité magnétique des argilites callovo-oxfordiennes de l'Est du Bassin


- de Paris: application à la recherche de hiatus sédimentaires. Ph.D. Thesis, Université Pierre et Marie Curie, Paris, p. 321.
- Husson, D., Galbrun, B., Laskar, J., Hinnov, L.A., Locklair, R., 2011. Astronomical calibration of the Maastrichtian. *Earth and Planetary Science Letters* 305, 328–340.
- Ikeda, M., Tada, R., Sakuma, H., 2010. Astronomical cycle origin of bedded chert: a middle Triassic bedded chert sequence, Inuyama, Japan. *Earth and Planetary Science Letters* 297, 369–378.
- Imbrie, J., Imbrie, K.P., 1979. *Ice Ages: Solving the Mystery*. Macmillan, London, p. 224.
- Imbrie, J., Hays, J.D., Martinson, D.G., McIntyre, A., Mix, A.C., Morley, J.J., Pisias, N.G., Prell, W.L., Shackleton, N.J., 1984. The orbital theory of Pleistocene climate: support from a revised chronology of the marine  $\delta^{18}\text{O}$  record. In: Berger, A.L., Imbrie, J., Hays, J., Kukla, G., Saltzman, B. (Eds.), *Milankovitch and Climate, Part I*. D. Riedel, Dordrecht, pp. 269–305.
- Ito, T., Kumazawa, M., Hamano, Y., Matsui, T., Masuda, K., 1993. Long term evolution of the solar insolation variation over 4 Ga. *Proceedings of the Japan Academy, Series B: Physical and Biological Sciences* 69, 233–237.
- Ito, T., Masuda, K., Hamano, H., Matsui, T., 1995. Climate friction: a possible cause for secular drift of Earth's obliquity. *Journal of Geophysical Research* 100 (B8), 15147–15161.
- Jovane, L., Sprovieri, M., Coccioni, R., Florindo, F., Marsili, A., Laskar, J., 2010. Astronomical calibration of the middle Eocene Contessa Highway section (Gubbio, Italy). *Earth and Planetary Science Letters* 298, 77–88.
- Kent, D.V., 1999. Orbital tuning and geomagnetic polarity timescales. *Philosophical Transactions, Royal Society of London, Series A* 357, 1995–2007.
- Kent, D.V., Olsen, P.E., 2008. Early Jurassic magnetostratigraphy and paleolatitudes from the Hartford continental rift basin (eastern North America): testing for polarity bias, and abrupt polar wander in association with the central Atlantic magmatic province. *Journal of Geophysical Research* 113, B06105. doi: 10.1029/2007JB005407.
- Kim, J.C., Lee, Y.I., 1998. Cyclostratigraphy of the Lower Ordovician Dumugol Formation, Korea: meter-scale cyclicity and sequence-stratigraphic interpretation. *Geoscience Journal* 2, 134–147.
- Köppen, W., Wegener, A., 1924. *Die Klimate der geologischen Vorzeit*. Bornträger, Berlin, p. 256.
- Kozur, H.W., Bachmann, G.H., 2005. Correlation of the Germanic Triassic with the international scale. *Albertiana* 32, 21–35.
- Kuiper, K.F., Deino, A., Hilgen, F.J., Krijgsman, W., Renne, P.R., Wijbrans, J.R., 2008. Synchronizing rock clocks of Earth history. *Science* 320, 500–504.
- Lanci, L., Muttoni, G., Erba, E., 2010. Astronomical tuning of the Cenomanian Scaglia Bianca Formation at Furlo, Italy. *Earth and Planetary Science Letters* 292, 231–237.
- Laskar, J., 1990. The chaotic motion of the solar system: a numerical estimate of the size of the chaotic zones. *Icarus* 88, 266–291.
- Laskar, J., 1994. Large scale chaos in the Solar System. *Astronomy and Astrophysics* 287, L9–L12.
- Laskar, J., 1999. The limits of Earth orbital calculations for geological time-scale use. *Philosophical Transactions of the Royal Society of London, Series A* 357 1785–1759.
- Laskar, J., 2003. Chaos in the Solar System. *Annales Henri Poincaré* 4 (Suppl. 2), S693–S705.
- Laskar, J., 2006. Astronomical limits in using orbital tuning methodology for the Geologic Time Scale. 11<sup>th</sup> international Congress, International Association for Mathematical Geology Liege, Belgium, 3–8 September.
- Laskar, J., Quinn, T., Tremaine, S., 1992. Confirmation of resonant structure in the Solar System. *Icarus* 95, 148–152.
- Laskar, J., Joutel, F., Boudin, F., 1993a. Orbital, precessional and insolation quantities for the Earth from –20 Myr to +10 Myr. *Astronomy and Astrophysics* 270, 522–533.
- Laskar, J., Joutel, J., Robutel, P., 1993b. Stabilization of the Earth's obliquity by the Moon. *Nature* 361, 615–617.
- Laskar, J., Robutel, P., Joutel, J., Gastineau, M., Correia, A.C.M., Levrard, B., 2004. A numerical solution for the insolation quantities of the Earth. *Astronomy and Astrophysics* 428, 261–285.
- Laskar, J., Fienga, A., Gastineau, M., Manche, H., 2011. La2010: a new orbital solution for the long term motion of the Earth. *Astronomy and Astrophysics*, 532. doi: 10.1051/0004-6361/201116836.
- Levrard, B., Laskar, J., 2003. Climate friction and the Earth's obliquity. *Geophysical Journal International* 154, 970–990.
- Liebrand, D., Lourens, L., Hodell, D.A., de Boer, B., van de Wal, R.S.W., Pälike, H., 2011. Antarctic ice sheet and oceanographic response to eccentricity forcing during the early Miocene. *Climate of the Past* 7, 869–880.
- Locklair, R.E., Sageman, B.B., 2008. Cyclostratigraphy of the Upper Cretaceous Niobrara Formation, Western Interior, USA: a Coniacian-Santonian orbital timescale. *Earth and Planetary Science Letters* 269, 539–552.
- Lourens, L., Antonarakou, A., Hilgen, F.J., Van Hoof, A.A.M., Vergnaud-Grazzini, C., Zachariasse, W.J., 1996. Evaluation of the Plio-Pleistocene astronomical timescale. *Paleoceanography* 11 (4), 391–413.
- Lourens, L.J., Wehausen, R., Brumsack, H.J., 2001. Geological constraints on tidal dissipation and dynamical ellipticity of the Earth over the past three million years. *Nature* 409, 1029–1033.
- Lourens, L.J., Hilgen, F., Shackleton, N.J., Laskar, J., Wilson, D., 2004. The Neogene Period. In: Gradstein, F., Ogg, J., Smith, A. (Eds.), *A Geologic Time Scale 2004*. Cambridge University Press, Cambridge, pp. 400–440.
- Lourens, L.J., Sluijs, A., Kroon, D., Zachos, Z.C., Thomas, E., Röhl, U., Bowles, J., Raffi, I., 2005. Astronomical pacing of late Palaeocene to early Eocene global warming events. *Nature* 435, 1083–1087.
- Lyell, C., 1867. *Principles of Geology*. Vol. 1, tenth ed. John Murray, London, p. 670.
- Matthews, R.K., Frohlich, C., Duffy, A., 1997. Orbital forcing of global change throughout the Phanerozoic: a possible stratigraphic solution to the eccentricity phase problem. *Geology* 25, 807–810.
- Menning, M., Gast, R., Hagdorn, H., Kading, K.-C., Simon, T., Szurlies, M., Nitsch, E., 2005. Zeitskala für Perm und Trias in der Stratigraphischen Tabelle von Deutschland 2002, zyklusstratigraphische Kalibrierung von höherer Dyas und Germanischer Trias und das Alter der Stufen Radium bis Rhaetium 2005. In: Menning, M., Hendrich, A. (Eds.), *Erläuterungen zur Stratigraphischen Tabelle von Deutschland*. Newsletters of Stratigraphy, 41(1/3), pp. 173–210.
- Meyers, S., Sageman, B., Hinnov, L.A., 2001. Integrated quantitative stratigraphy of the Cenomanian-Turonian Bridge Creek Limestone member using evolutive harmonic analysis and stratigraphic modeling. *Journal of Sedimentary Research* 71, 627–643.
- Meyers, S., Siewert, S.E., Singer, B.S., Sageman, B.B., Condon, D.J., Obradovich, J.D., Jicha, B.R., and Sawyer, D.A., in press. Intercalibration of radioisotopic and astrochronologic time scales for the Cenomanian-Turonian Boundary interval, Western Interior Basin, USA. *Geology*.

- Milankovitch, M., 1941. Kanon der Erdbestrahlung und seine Anwendung auf das Eiszeitenproblem. Royal Serbian Academy, Section of Mathematical and Natural Sciences, Belgrade, p. 633 [and 1998 reissue in English: *Canon of Insolation and the Ice-Age Problem*. Belgrade: Serbian Academy of Sciences and Arts, Section of Mathematical and Natural Sciences, 634 pp.].
- Min, K., Mundil, R., Renne, P.R., Ludwig, K.R., 2000. Systematic errors in  $^{40}\text{Ar}/^{39}\text{Ar}$  geochronology through comparison with U/Pb analysis of a 1.1-Ga rhyolite. *Geochimica et Cosmochimica Acta* 64, 73–98.
- Mitchell, R.N., Bice, D.M., Montanari, A., Cleaveland, L.C., Christianson, K.T., Coccioni, R., Hinnov, L.A., 2008. Ocean anoxic cycles? Prelude to the Livello Bonarelli (OAE 2). *Earth and Planetary Science Letters* 267, 1–16.
- Mourik, A.A., Bijkerk, J.F., Cascella, A., Hüsing, S.K., Hilgen, F.J., Lourens, L.J., Turco, E., 2010. Astronomical tuning of the La Vedova High Cliff section (Ancona, Italy)—implications of the middle Miocene Climate Transition for Mediterranean sapropel formation. *Earth and Planetary Science Letters* 297, 249–261.
- Munk, W., 1997. Once again: once again—tidal friction. *Progress in Oceanography* 40, 7–35.
- Nestor, H., Einasto, R., Nestor, V., Marss, T., Viira, V., 2001. Description of the type section, cyclicity and correlation of the Riksu Formation (Wenlock, Estonia). *Proceedings of the Estonian Academy of Sciences, Geology* 50, 149–173.
- Nestor, H., Einasto, R., Mannik, P., Nestor, V., 2003. Correlation of lower-middle Llandovery sections in central and southern Estonia and sedimentation cycles of lime muds. *Proceedings of the Estonian Academy of Sciences, Geology* 52, 3–27.
- Ogg, J.G., Gradstein, F.M., Lugowski, A., Ault, A., 2011. TimeScale Creator Available at: <http://www.tscreeator.org>.
- Olsen, P.E., Kent, D.V., 1996. Milankovitch climate forcing in the tropics of Pangea during the Late Triassic. *Palaeogeography Palaeoclimatology Palaeoecology* 122, 1–26.
- Olsen, P.E., Kent, D.V., 1999. Long-period Milankovitch cycles from the Late Triassic and Early Jurassic of eastern North America and their implications for the calibration of the Early Mesozoic time-scale and the long-term behaviour of the planets. *Philosophical Transactions of the Royal Society of London, Series A* 357, 1761–1786.
- Osleger, D.A., 1995. Depositional sequences on Upper Cambrian carbonate platforms: variable sedimentologic responses to allogenic forcing. In: Haq, B.U. (Ed.), *Sequence Stratigraphy and Depositional Responses to Eustatic, Tectonic and Climate Forcing*. Kluwer Academic Publishers, Dordrecht, pp. 247–276.
- Paillard, D., Labeyrie, L., Yiou, P., 1996. Macintosh program performs time-series analysis. *Eos* 77, 379.
- Pälike, H., Shackleton, N.J., 2000. Constraints on astronomical parameters from the geological record for the last 25 Myr. *Earth and Planetary Science Letters* 182, 1–14.
- Pälike, H., Shackleton, N.J., Röhl, U., 2001. Astronomical forcing in Late Eocene marine sediments. *Earth and Planetary Science Letters* 193, 589–602.
- Pälike, H., Laskar, J., Shackleton, N.J., 2004. Geological constraints on the chaotic diffusion of the Solar System. *Geology* 32, 929–932.
- Pälike, H., Norris, R.D., Herrle, J.O., Wilson, P.A., Coxall, H.K., Lear, C.H., Shackleton, N.J., Tripathi, A.K., Wade, B.S., 2006. The heartbeat of the Oligocene climate system. *Science* 314, 1894–1898.
- Petit, J.R., Jouzel, J., Raynaud, D., Barkov, N.I., Barnola, J.-M., Basile, I., Bender, M., Chappellaz, J., Davis, M., Delaygue, G., Delmotte, M., Kotlyakov, V.M., Legrand, M., Lipenkov, V.Y., Lorius, C., Pépin, L., Ritz, C., Saltzman, E., Stievenard, M., 1999. Climate and atmospheric history of the past 420,000 years from the Vostok ice core, Antarctica. *Nature* 399, 429–436.
- Prokopenko, A.A., Karabanov, E.B., Williams, D.F., Kuzmin, M.I., Shackleton, N.J., Crowhurst, S.J., Peck, J.A., Gvozdkov, A.N., King, J.W., 2001. Biogenic silica record of the Lake Baikal response to climatic forcing during the Brunhes. *Quaternary Research* 55, 123–132.
- Ray, R.D., Eanes, R.J., Lemoine, F.G., 2001. Constraints on energy dissipation in the Earth's body tide from satellite tracking and altimetry. *Geophysical Journal International* 144, 471–480.
- Renne, P.R., Deino, A.L., Walter, R.C., Turrin, B.D., Swisher, C.C., Becker, T.A., Curtis, G.H., Sharp, W.D., Jaouni, A.-R., 1994. Intercalibration of astronomical and radioisotopic time. *Geology* 22, 783–786.
- Renne, P.R., Swisher, C.C., Deino, A.L., Karner, D.B., Owens, T., DePaolo, D.J., 1998. Intercalibration of standards, absolute ages and uncertainties in  $^{40}\text{Ar}/^{39}\text{Ar}$  dating. *Chemical Geology* 145, 117–152.
- Renne, P.R., Mundil, R., Balco, G., Min, K., Ludwig, K.R., 2010. Joint determination of  $^{40}\text{K}$  decay constants and  $^{40}\text{Ar}^*/^{40}\text{K}$  for the Fish Canyon sanidine standard, and improved accuracy for  $^{40}\text{Ar}/^{39}\text{Ar}$  geochronology. *Geochimica et Cosmochimica Acta* 74, 5349–5367.
- Rivera, T.A., Storey, M., Zeeden, C., Hilgen, F., and Kuiper, K., in press. A refined astronomically calibrated  $^{40}\text{Ar}/^{39}\text{Ar}$  age for Fish Canyon sanidine. *Earth and Planetary Science Letters*.
- Rodionov, V.P., Dekkers, M.J., Khramov, A.N., Gurevich, E.L., Krijgsman, W., Duermeijer, C.E., Heslop, D., 2003. Paleomagnetism and cyclostratigraphy of the Middle Ordovician Krivolutsky Suite, Krivaya Luka section, southern Siberian Platform: record of non-synchronous NRM-components for a non-axial geomagnetic field? *Studia Geophysica et Geodaetica* 47, 255–274.
- Rubincam, D.P., 1994. Insolation in terms of Earth's orbital parameters. *Theoretical and Applied Climatology* 48, 195–202.
- Rubincam, D.P., 1995. Has climate changed the Earth's tilt? *Paleoceanography* 10, 365–372.
- Ruhl, M., Deenen, M.H.L., Abels, H.A., Bonis, N.R., Krijgsman, W., Kürschner, W.M., 2010. Astronomical constraints on the duration of the early Jurassic Hettangian stage and recovery rates following the end-Triassic mass extinction (St. Audrie's Bay/East Quantoxhead, UK). *Earth and Planetary Science Letters* 295, 262–276.
- Schwarzacher, W., 1947. Über die sedimentäre Rhythmik des Dachsteinkalkes von Lofer. *Verhandlung der Geologische Bundesanstalt, Wien* 1947, 175–188.
- Schwarzacher, W., 1954. Die Grossrhythmik des Dachsteinkalkes von Lofer. *Tschermaks Mineralogische und Petrographische Mitteilungen* 4, 44–54.
- Schwarzacher, W., 1993. Cyclostratigraphy and the Milankovitch Theory. *Developments in Sedimentology* 54, 225.
- Shackleton, N., 1967. Oxygen isotope analyses and Pleistocene temperatures re-assessed. *Nature* 215, 15–17.
- Shackleton, N.J., Berger, A., Peltier, W.A., 1990. An alternative astronomical calibration of the lower Pleistocene time scale based on ODP Site 677. *Transactions of the Royal Society of Edinburgh—Earth Sciences* 81, 251–261.
- Shackleton, N.J., Crowhurst, S., Hagelberg, T., Pisias, N.G., Schneider, D.A., 1995. A new Late Neogene time scale: application to Leg 138 Sites. *Proceedings of the ODP, Scientific Results* 138, 73–101.
- Shackleton, N.J., Crowhurst, S.J., Weedon, G.P., Laskar, J., 1999. Astronomical calibration of Oligocene-Miocene time. *Royal Society of London Philosophical Transactions, series A* 357, 1907–1929.

- Siewert, S.E., Singer, B.S., Condon, D., Meyers, S.R., Sageman, B.B., Jicha, B.R., Obradovich, J., Sawyer, D.A., 2011. Integrating Astrochronology of the Upper Cretaceous Niobrara Formation with  $^{40}\text{Ar}/^{39}\text{Ar}$  and U-Pb Geochronology. 2011 UW-Madison Geoscience Graduate Symposium 27<sup>th</sup> April, Oral presentation.
- XSimonson, B.M., Hassler, S.W., 1996. Was the deposition of large Precambrian iron formations linked to major transgressions? *Journal of Geology* 104, 665–676.
- Smith, M.E., Chamberlain, K.R., Singer, B.S., Carroll, A.R., 2010. Eocene clocks agree: coeval  $^{40}\text{Ar}/^{39}\text{Ar}$ , U-Pb, and astronomical ages from the Green River Formation. *Geology* 38, 527–530.
- Sprenger, A., Ten Kate, J., 1993. Orbital forcing of calcilutite-marl cycles in southeast Spain and an estimate for the duration of the Berriasian stage. *Geological Society of America Bulletin* 105, 807–818.
- Sprovieri, M., Coccioni, R., Lirer, F., Pelosi, N., Lozar, F., 2006. Orbital tuning of a lower Cretaceous composite record (Maiolica Formation, central Italy). *Paleoceanography* 21, PA4212. doi:10.1029/2005PA001224.
- Strasser, A., 2007. Astronomical time scale for the Middle Oxfordian to Late Kimmeridgian in the Swiss and French Jura Mountains. *Swiss Journal of Geosciences* 100, 407–429.
- Suan, G., Pittet, B., Bour, I., Mattioli, E., Duarte, L.V., Mailliot, S., 2008. Duration of the Early Toarcian carbon isotope excursion deduced from spectral analysis – consequence for its possible causes. *Earth and Planetary Science Letters* 267, 666–679.
- Sun, Y., Clemens, S.C., An, Z., Yu, Z., 2006. Astronomical timescale and palaeoclimatic implication of stacked 3.6-Myr monsoon records from the Chinese Loess Plateau. *Quaternary Science Reviews* 25, 33–48.
- Szurliés, M., 2004. Magnetostratigraphy: the key to global correlation of the classic Germanic Trias – case study Volpriehausen Formation (Middle Buntsandstein), Central Germany. *Earth and Planetary Science Letters* 227, 395–410.
- Szurliés, M., 2007. Latest Permian to Middle Triassic cyclo-magnetostratigraphy from the Central European Basin, Germany: implications for the geomagnetic polarity timescale. *Earth and Planetary Science Letters* 261, 602–619.
- Taner, M.T., 2000. Attributes revisited. Technical Publication, RockSolid Images, Inc, Houston, TX. Available from: [http://www.rocksolidimages.com/pdf/attrib\\_revisited.htm](http://www.rocksolidimages.com/pdf/attrib_revisited.htm).
- Taner, M.T., Koehler, F., Sheriff, R.E., 1979. Complex trace analysis. *Geophysics* 44 (6), 1041–1063.
- Tanner, L.H., 2010. Cyclostratigraphic record of the Triassic: a critical examination. *Geological Society of London, Special Publications* 334, 119–137.
- Thomson, D.J., 1982. Spectrum estimation and harmonic analysis. *IEEE Proceedings* 70, 1055–1096.
- Thomson, D.J., 1990. Quadratic-inverse spectrum estimates: applications to Palaeoclimatology. *Philosophical Transactions: Physical Sciences and Engineering* 332, 539–597.
- Tucker, M., Garland, J., 2010. High-frequency cycles and their sequence stratigraphic context: orbital forcing and tectonic controls on Devonian cyclicity, Belgium. *Geologica Belgica* 13, 213–240.
- Waelbroeck, C., Labeyrie, L., Michel, E., Duplessy, J.C., McManus, J.F., Lambeck, K., Blabon, E., Labracherie, M., 2002. Sea-level and deep water temperature changes derived from benthic foraminifera isotopic records. *Quaternary Science Reviews* 21, 295–305.
- Weedon, G.P., Jenkyns, H.C., 1999. Cyclostratigraphy and the Early Jurassic timescale: data from the Belemnite Marls, Dorset, southern England. *Geological Society of America Bulletin* 111, 1823–1840.
- Weedon, G.P., Jenkyns, H.C., Coe, A.L., Hesselbo, S.P., 1999. Astronomical Calibration of the Jurassic Time-scale from Cyclostratigraphy in British Mudrock Formations. *Philosophical Transactions of the Royal Society of London Series A* 357 (1757), 1787–1813.
- Weedon, G.P., Coe, A.L., Gallois, R.W., 2004. Cyclostratigraphy, orbital tuning and inferred productivity for the type Kimmeridge Clay (Late Jurassic), Southern England. *Journal of the Geological Society, London* 161, 655–666.
- Westerhold, T., Röhl, U., 2009. High resolution cyclostratigraphy of the early Eocene – new insights into the origin of the Cenozoic cooling trend. *Climate of the Past* 5, 309–327.
- Westerhold, T., Röhl, U., Laskar, J., Bowles, J., Raffi, I., Lourens, L.J., Zachos, J.C., 2007. On the duration of magnetochrons C24r and C25n and the timing of early Eocene global warming events: implications from the Ocean Drilling Program Leg 208 Walvis Ridge depth transect. *Paleoceanography* 22, PA2201. doi: 10.1029/2006PA001322.
- Westerhold, T., Röhl, U., Raffi, I., Fornaciari, E., Monechi, S., Reale, V., Bowles, J., Evans, H.F., 2008. Astronomical calibration of the Paleocene time. *Palaeogeography, Palaeoclimatology, Palaeoecology* 257, 377–403.
- Westerhold, T., Röhl, U., McCarren, H.K., Zachos, J.C., 2009. Latest on the absolute age of the Paleocene-Eocene Thermal Maximum (PETM): new insights from exact stratigraphic position of key ash layers +19 and –17. *Earth and Planetary Science Letters* 287, 412–419.
- Whiteside, J.H., Olsen, P.E., Eglinton, T., Brookfield, M.E., Sambrotto, R.N., 2010. Compound-specific carbon isotopes from Earth's largest flood basalt eruptions directly linked to the end-Triassic mass extinction. *Proceedings of the National Academy of Sciences* 107 (5), 6721–6725.
- Williams, G.E., 2000. Geological constraints on the Precambrian history of Earth's rotation and the Moon's Orbit. *Reviews of Geophysics* 38, 37–59.
- Williams, D.F., Peck, J., Karabanov, E.B., Prokopenko, A.A., Kravchinsky, V., King, J., Kuzmin, M.I., 1997. Lake Baikal record of continental climate response to orbital insolation during the past 5 million years. *Science* 297, 1114–1117.
- Wotzlaw, J., Schaltegger, U., Kuiper, K., Guenter, D., 2010. Deriving accurate eruption ages from complex zircon populations: insights from zircon trace element chemistry and intercalibration with astronomical time. *American Geophysical Union Fall Meeting San Francisco*, 13–17 December, abstract #V31A–2312.
- Ziółkowski, P., Hinnov, L.A., 2010. High-resolution cyclostratigraphic analysis of the magnetic susceptibility record from the Upper Bajocian to Upper Bathonian of Central Poland and the mineralogical link between magnetic susceptibility and palaeoclimatic changes. 8<sup>th</sup> International Congress on the Jurassic System Sichuan, China, 9–13 August, abstract.



## AUTHOR QUERY FORM

	<p><b>Book:</b> GRADSTEIN-9780444594259</p> <p><b>Chapter:</b> 04</p>	<p><b>Please e-mail your responses and any corrections to:</b>  <b>E-mail: P.Wilkinson@Elsevier.com</b></p>
---	---	---

Dear Author,

Any queries or remarks that have arisen during the processing of your manuscript are listed below and are highlighted by flags in the proof. (AU indicates author queries; ED indicates editor queries; and TS/TY indicates typesetter queries.) Please check your proof carefully and answer all AU queries. Mark all corrections and query answers at the appropriate place in the proof (e.g., by using on-screen annotation in the PDF file [http://www.elsevier.com/framework\\_authors/tutorials/ePDF\\_voice\\_skin.swf](http://www.elsevier.com/framework_authors/tutorials/ePDF_voice_skin.swf)) or compile them in a separate list, and tick off below to indicate that you have answered the query.

**Please return your input as instructed by the project manager.**

<p><b>Uncited reference:</b> References that occur in the reference list but are not cited in the text. Please position each reference in the text or delete it from the reference list.          The following are not cited Prokopenko et al., 2001</p>	
<p><b>Missing reference:</b> References listed below were noted in the text but are missing from the reference list. Please make the reference list complete or remove the references from the text.          NIL</p>	
Location in Chapter	Query / Remark
AU:1, page 77	Should these have 40 and 39 superscripts? <span style="float: right;"><input type="checkbox"/></span>
AU:2, page 71	Please insert table title? <span style="float: right;"><input type="checkbox"/></span>
AU:3, page 76	Please insert table title? <span style="float: right;"><input type="checkbox"/></span>

**Abstract:**

The Milankovitch theory that quasi-periodic oscillations in the Earth-Sun position have induced significant  $10^4$ - $10^6$  year variations in the Earth's stratigraphic record of climate is widely acknowledged. This chapter summarizes the Earth's astronomical parameters, the nature of astronomically forced solar radiation, fossil astronomical signals in the stratigraphic record, and the use of these signals in calibrating geologic time.

**Keywords:** ■■■